FACULDADE DE ENGENHARIA DA UNIVERSIDADE DO PORTO

Intellwheels - Controlling an Intelligent Wheelchair using a Multimodal Interface

Patrícia Marques de Almeida

Mestrado Integrado em Bioengenharia

Supervisor: Professor Luís Paulo Gonçalves dos Reis

Co - Supervisor: Professora Brígida Mónica Faria

July 27, 2021

Resumo

A independência e autonomia tanto dos idosos como das pessoas com deficiência tem sido uma preocupação crescente da sociedade atual. Assim sendo, as cadeiras de rodas têm demonstrado ser fundamentais para a deslocação destas pessoas com deficiências físicas nos membros inferiores, paralisias ou outro tipo de doenças limitadoras.

Consequentemente, o aumento da esperança de vida acompanhado pelo envelhecimento da população criou as condições ideais para o nascimento de um novo conceito de cadeira de rodas, Cadeira de Rodas Inteligente. Desenvolvendo-se assim uma nova forma de navegação, mais personalizável e de fácil uso, aumentando a inclusão e, por conseguinte, melhorando a qualidade de vida de todos aqueles que apresentam alguma restrição de mobilidade.

Deste modo, diversos sensores adaptados devem ser utilizados para se potencializar o controlo de uma cadeira de rodas. Durante este trabalho analisaram-se dois sensores, o Leap Motion e o NeuroSky Mindwave Mobile 2, para converter a vontade do utilizador num de quatro comandos de condução fundamentais, seguir em frente, virar à direita, esquerda ou parar.

O Leap Motion pretende determinar a direção a seguir consoante o gesto da mão identificado. Para isso nesta prova de conceito foram recolhidos dados de voluntários enquanto executavam os gestos definidos. Assim foi possível criar um conjunto de dados que depois de processado e extraídas algumas características permitiu obter uma classificação dos dados com um F1-Score superior a 0.97. Para além disso este sensor quando testado numa aplicação em tempo real reforçou o seu elevado desempenho.

O NeuroSky Mindwave Mobile 2 permite recolher ondas cerebrais nas quais é possível reconhecer ritmos associados à imaginação de determinadas ações. De acordo com isto, foram realizadas aquisições de dados enquanto pessoas imaginavam as direções sob quatro condições diferentes. Numa primeira abordagem os participantes deveriam imaginar as direções depois de observar uma imagem representativa da mesma. Numa segunda parte observavam um vídeo de uma cadeira de rodas a executar determinados movimentos ao mesmo tempo que deveriam imaginar essa ação. A terceira aquisição, muito semelhante à segunda, no entanto o vídeo observado pretendia verificar se a direção podia ser mais facilmente identificada se o vídeo mostrasse as mesmas direções a serem executadas de uma forma mais rápida e violenta, como uma montanha-russa. Por último, recolheram-se dados quando os voluntários percorriam um trajeto predefinido usando uma cadeira de rodas.

Destes 4 conjuntos de dados, o que corresponde a imaginar a direção pretendida depois de ser mostrada a respetiva seta da direção, ou seja, o primeiro conjunto de dados, foi aquele que demonstrou ser mais eficaz na classificação.

Abstract

The independence and autonomy of both elderly and disabled people has been a growing concern of today's society. Therefore, wheelchairs have proven to be fundamental for the movement of these people with physical disabilities in the lower limbs, paralysis or other type of restrictive diseases.

Consequently, the increase in life expectancy combined with the ageing of the population has created the ideal conditions for the introduction of a new wheelchair concept, the Intelligent Wheelchair. Hence, a new form of navigation, more customizable and easy to use, promoting inclusion and subsequently enhancing the quality of life of everyone with some mobility restriction, has been developed.

For this purpose, several adapted sensors should be used to optimize the control of a wheelchair. During this work, two sensors, Leap Motion and NeuroSky Mindwave Mobile 2, were analyzed to convert the user's will into one of four fundamental driving commands, move forward, turn right, left, or stop.

Leap Motion aims to determine the direction to follow according to the hand gesture identified. For this task, in this proof of concept, data was collected from volunteers while they were performing certain gestures. Thereby it was possible to produce a data set that after being processed and extracted some features enabled classification of the data with an F1-Score higher than 0.97. Additionally, when tested in a real-time application, this sensor reinforced its high performance.

The NeuroSky Mindwave Mobile 2 sensor is able to collect brain waves in which it is possible to recognize rhythms associated with imagining certain actions. Accordingly, data acquisitions were performed while people imagined the directions under four different conditions. In a first approach, participants were supposed to imagine the directions after observing a representative image of it. In a second part, they watched a video of a wheelchair performing particular movements at the same time as they were supposed to imagine that action. The third acquisition, very similar to the second one, however, the watched video was intended to verify if the direction could be more easily identified when the video showed the same directions being executed in a faster and more violent manner, for instance in a roller-coaster. Lastly, data were collected when the volunteers followed a predefined route using a wheelchair.

Among these 4 data sets, the one that corresponds to imagining the desired direction after being displayed the respective cue, in other words, the first data set, was the one that proved to be most effective in classification.

Agradecimentos

Esta dissertação representa o culminar de muitos anos de trabalho nos quais tive possibilidade de me cruzar com diversas pessoas às quais gostava de deixar um sincero agradecimento.

Primeiro, ao professor Luís Paulo Reis e professora Brígida Mónica Faria bem como a todo o grupo Intellwheels que me acolheu, agradeço toda a ajuda, ensinamentos e apoio prestado nestes últimos meses. Aproveito também para deixar uma palavra de apreço a todos aqueles que despenderam do seu tempo para serem voluntários neste estudo.

Em segundo lugar, quero agradecer a todas as pessoas das mais diversas áreas, desde a professora primária que fazia quilómetros e quilómetros só para nos vir dar aulas, a todos os motoristas que durante anos percorreram a 'serra' para nos levarem à escola. Todos tiveram um papel importante na minha formação, acrescentaram-me valor e mostraram-me que podemos ter desafios, mas que somos capazes de os superar.

Em terceiro, pelos valores transmitidos, experiências vividas e impacto pessoal deixo o meu agradecimento a todos os que conviveram comigo e me permitiram crescer, aprender e valorizar apenas o essencial na grande escola da vida que foi e continua a ser, o Escutismo.

Posteriormente, a todos meus amigos, desde os mais antigos aos que a universidade me deu, agradeço por me terem permitido acreditar e alinharem comigo nas mais diversas aventuras.

Por último, mas não menos importante, deixar um especial obrigado à minha família, nomeadamente pais e irmãos que sempre me acompanharam, ajudaram e apoiaram durante todo este percurso.

Assim e porque não foi de forma nenhuma um caminho solitário reforço o meu obrigada, com vocês esta jornada tornou-se mais fácil e enriquecedora.

Muito Obrigado,

Patrícia Almeida

" Começa onde estás.
Usa o que tens.
Faz o que puderes."

Arthur Ashe

Contents

List of Figures

List of Tables

Abbreviations and Symbols

ANC	Activity of Neural Cells
ApEn	Approximate entropy
API	Application Programming Interface
ATs	Assistive Technologies
BCI	Brain-Computer Interfaces
BMI	Brain–Machine Interfaces
FD	Fractal Dimension
D_p	First Difference of IMF's Phase
D_t	First Difference of IMF Time Series
DT	Decision Tree
ECG	Electrocardiography
EMD	Empirical Mode Decomposition
EMG	Electromyography
E_{norm}	Normalized Energy of IMF
EOG	Electrooculography
ERD	Event-Related Desynchronization
ERP	Event-Related Potentials
ERS	Event-Related Synchronization
FN	False Negative
FP	False Positive
GNB	Gaussian Naïve Bayes
HMI	Human Machine Interface
IMFs	Intrinsic Mode Functions
IoT	Internet of Things
ISO	International Organization for Standardization
IW	Intelligent Wheelchairs
K-NN	K-Nearest Neighbours
LDA	Linear Discriminant Analysis
LIACC	Artificial Intelligence and Computer Science Laboratory
LR	Logistic Regression
MI	Motor-Imagery
MLP	Multilayer Perceptron
PCA	Principal Component Analysis
PE	Permutation entropy
PPG	Photoplethysmography
PSD	Power Spectral Density
PW	Powered Wheelchairs
RF	Random Forest

SampEn	Sample Entropy
SDK	Software Development Kit
SE	Spectral entropy
SSEP	Steady-State Evoked Potential
SSVEP	Steady-State Visually Evoked Potential
SVDE	Singular Value Decomposition Entropy
SVM	Support Vector Machine
SW	Smart Wheelchairs
TGC	ThinkGear Connector
TN	True Negative
TP	True Positive
WHO	World Health Organization

Chapter 1

Introduction

1.1 Motivation

Independence and autonomy in mobility are two of the most important conditions for determining the quality of life of people with disabilities or with low mobility capacities [1]. Limited mobility could have origin in a broad range of situations, from accidents to disease, to the ageing process.

Currently, several mobility related technologies were designed to achieve an independent mobility, in particular powered orthosis, prosthetic devices, and exoskeletons. Notwithstanding these devices, wheeled mobility devices remain among the most used assistive devices [2].

According to World Health Organization (WHO) [3], approximately 10% of the world's population, or around 740 million people, suffer from disabilities and between those people, almost 10% require a wheelchair. Therefore, it is estimated that about 1% of the total population needs wheelchairs, which translates into 74 million people worldwide [4].

The importance of providing multifaceted wheelchairs which can be adapted to the most diverse conditions of their users is thus emphasised. Different interfaces are being developed enabling to overcome existing barriers of use. In particular, special attention has been dedicated to voice control techniques, joysticks, tongue or head movements. However, hand gesture recognition and brain-computer interface (BCI) systems are proving to be extremely successful methods of wheelchair control due to their accessible price and non-invasiveness.

1.2 Objectives

The development of new types of interaction between humans and machines to ensure more equality and simplicity in the use of devices is one of the concerns of biomedical engineering.

The use of BCI will enable those who have suffered from various diseases, namely Amyotrophic Lateral Sclerosis and Spinal cord injuries, to restore some of their mobility and become responsible for their own movements again.

Hand gestures are usually taken for granted, but unfortunately not everyone has the same dexterity to perform these movements. For example, people who are affected by a stroke or have

radial nerve injury could have their wrist flexion and extension movements affected. Besides, there are also amputees who are unable to control a joystick properly. Therefore, solutions providing hand/wrist movements which are personalised or adapted to each person and their health condition play a fundamental role in the path to independence.

The present study intends to introduce insights into this field of intelligent wheelchairs in order to overcome this perceived problem.

Concerning this document, it has the main purpose of expanding the knowledge about the notion of wheelchairs and analysing possible alternatives to be integrated in an IW control system. For that, some important wheelchair prototypes already developed are initially described. Afterwards the state of the art related to adaptive sensors for hand gestures and sensors capable of recording the user's brain activity is presented. Lastly, a preliminary study on data obtained with two of the sensors is described.

1.3 Document Structure

Besides this Introduction chapter, the document comprises five more chapters. The first one (Chapter 2) presents the concepts of Assistive Technologies and Intelligent Wheelchairs and some relevant prototypes in wheelchair domain.

Thereafter, adaptive sensors will be described in Chapter 3. This chapter also incorporates a state of art focused on Sensors for Hand Gesture Detection and EEG Sensors due to the fact that these are the ones intended to be used during the practical experiments.

In Chapter 4, a proposed solution, methodology and work developed can be found.

The following chapter (Chapter 5) aggregates the results obtained for each of the studied sensors.

Finally, some conclusions and considerations concerning this dissertation are explained in Chapter 6.

Chapter 2

Assistive Technologies

In this chapter the concept of Assistive Technologies will be discussed, namely one of the assistive technologies for mobility. More in detail, this chapter will include the Intelligent Wheelchair concept and how it has evolved over time.

2.1 Assistive Technologies Concept

Assistive Technologies (ATs) are products for assisting and improving the quality of life of people affected by a wide range of health conditions, namely the elderly and people with disabilities [5].

According to the International Organization for Standardization (ISO), an assistive product corresponds to any product (including devices, equipment, instruments and software), specially produced or generally available, used by or for people with disabilities [6]. Thus, ATs facilitate self-care, minimize health costs and promote independence and well-being in people with cognitive and physical limitations. Therefore, the functionalities of ATs can range from devices that compensate body function impairments, to those that promote inclusion in social activities.

The classification and organization of those technologies is not as evident as their importance to society. Some authors have proposed a division based on the functionality of human activity, highlighting four areas - mobility, communication, manipulation and orientation [7]. Donelly, 2008 [8] and Blackhurst, 2005 [9] suggested an organization in seven areas, depending on the origin of the problem (life maintenance, communication, body stabilization, mobility, daily activities, education and hobbies). While Nunes, 2012 [10] distinguished two categories according to the type of accessibility that ATs provides: digital or physical.

2.2 Intelligent Wheelchairs

The independence and autonomy of both the elderly and people with disabilities has been an increasing concern of today's society. Taking this into consideration, wheelchairs are an important means of travel for people with lower limb physical disabilities and senior citizens [11]. The increase in life expectancy accompanied by the ageing of the population led to the emerging of

the new concept of wheelchair - Intelligent Wheelchair (IW) [12]. This new equipment will allow safe navigation avoiding obstacles using an intelligent, easy and adaptable user interface and communication with other devices.

2.2.1 Concept

The notion of wheelchair remote to its physical appearance once it is normally composed by a chair fitted with wheels. Initially, wheelchairs were manually operated devices designed for use by a person with a mobility disability for the main purpose of indoor or both, indoor and outdoor locomotion [13]. Over time, wheelchairs are considered as powerful resources to overcome critical limitations and disabilities resulting from several types of handicaps and illnesses [14], and for this reason this device was investigate and some new concepts appeared, particularly the Powered Wheelchairs (PW) and Intelligent Wheelchairs or Smart Wheelchairs (SW).

The first one, PW, is a device that may be propelled using motors; however, safe operation of PW requires a sufficient level of cognitive capacity, including decision-making, memory and self-awareness [15, 16].

The second and most recent, IW, emerges from the need to improve the traditional features of the wheelchair to obtain a more inclusive device. This new equipment uses degrees of intelligent systems that, while reducing the weaknesses of previous versions of wheelchairs, further improves the users' ability to control them [17]. Typically, an IW consists of a computer and a set of sensors. The computer is responsible for controlling the IW using the information collected by the sensors. This control can be automatic, if only the output processed from the sensors is used, or it can be shared, in which an interface control such as a joystick, voice commands, facial expressions or even eye movement is required [18]. Succinctly, IW stands out for its navigation capabilities and automatic adaptation of their interface to the user [14].

All studies in this area aim to discover and develop an appropriate wheelchair, this means a wheelchair that meets the individual's needs and environmental conditions; provides an appropriate fit and postural support; is safe and durable; can help open a new world for the user, from exclusion to inclusion, participation in all activities of society, sports and recreation, which leads to independence, better health and quality of life [19].

2.2.2 Prototypes

The first wheelchairs schemes were considered to appear on 1595, made by an unknown inventor for Philip II [14]. However, it was only after the early 1980s that intelligent wheelchairs were the subject of further research and so their first prototypes were released.

The figure 2.1 provides a timeline with some significant IWs projects.

Afterwards, these prototypes will be enumerated and their main characteristics described.

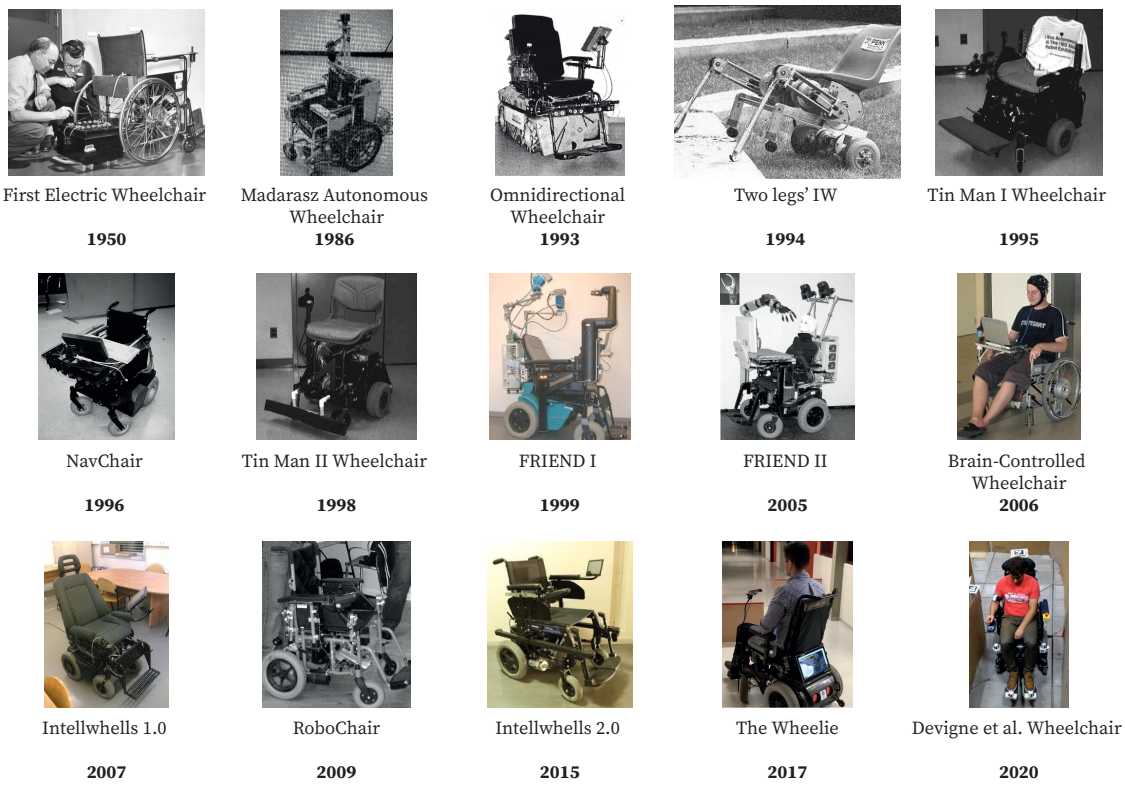

Figure 2.1: Intelligent Wheelchairs Prototypes (adapted from [14, 20–22])

1. **First Electric Wheelchair (1950)**

   In 1950, George Klein invented the first electric wheelchair. His goal was to support veterans returning home from the Second World War. This prototype was large, heavy, and ungainly [23].

2. **Madarasz Autonomous Wheelchair (1986)**

   Madarasz et al., 1986 [24] proposed an autonomous vehicle for physically disable people. This equipment was based on a self-navigation wheelchair with the main objective of transport a person from one location to another between crowded rooms in a building without requiring of human intervention.

   This prototype stands out from other autonomous vehicles for its unique characteristics, namely the possibility to operate inside an office and with minimum impact on the building in which it will be used. For these features, it needed to be equipped with a microcomputer, a digital camera and an ultrasound scanner. Through reference points collected, the camera recognized the surrounding environment and calculated the wheelchair location. Then, the obstacles are detected by the ultrasound scanner and the microcomputer operated using actuators, after processing all the information [24].

3. **Omnidirectional Wheelchair (1993)**

   Hoyer and Hölper, 1993 [25] created a high functional and flexible wheelchair. Since its control system (based on modular structures) is flexible configurable, it can be controlled in accordance with the needs of different users, thus allowing its use by people with severe or multiple physical disabilities. This equipment was highlighted for its path planning, tasks modules and its interface which recognized different types of inputs (voice, joystick and terminal control commands) [26, 27].

4. **Two legs' IW (1994)**

   In 1994, a new hybrid wheelchair emerged. Wellman et al. [28] developed a chair equipped with wheels and legs capable of walking in uneven terrain and circumventing obstacles, which facilitated some daily activities.

5. **NavChair (1996)**

   The NavChair Assistive Wheelchair developed in 1994 by Levine et al. [29] consisted of a commercial wheelchair system equipped with a DOS-based computer system, ultrasonic sensors and an interface module with joystick and a power module. It was noted for its three operating modes that enable it the avoidance of obstacles, door passage, and automatic wall tracking. Besides that, this IW had a control system shared between the system and user.

6. **Tin Man I Wheelchair (1995) & Tin Man II (1998)**

   During 1995 Miller and Slack [30] created the first version of the Tin Man wheelchair, a robotic wheelchair oriented approach. It has composed by five types of sensors: proximity infrared sensors, contact sensors, drive motor encoders, sonars range finders and Fluxgate compass. Regarding the operation modes, there were three possibilities: driving with automatic obstacle avoidance, moving along a previously defined path and moving from a starting point to an end point [31].

   Tin Man II appeared in 1998 as an evolution of the first prototype in order to eliminate previous failures, which means reducing the dependency on the contact sensor, improving the user interface, increasing the operating speed and creating a better system for user testing. Moreover, the capabilities to store travel information, return to the starting point, follow walls, go through doors and recharge battery were added [26, 30].

7. **FRIEND I (1999) & FRIEND II (2005)**

   Considering the disabled persons with upper-limb impairments, Borgerding et al. [32] conceived in 1999 a wheelchair to operate as a personal assistant to support these people. The model presented a MANUS manipulator and the control system of both, manipulator and wheelchairs, belongs to a complex control architecture with screen and voice commands as input interfaces [31].

A few years later, an upgrade of FRIEND I was made to increase the usability of service robots designed for paralyzed people with quadriplegia or similar disabilities. Those developments lead to FRIEND II prototype, a prototype able to interact with other smart devices. These improvements were achieved with the use of new camera systems, a human robot arm with 7 degrees of freedom, a Kinematic Configuration Control, a force torque sensor and two interchangeable clamps [33].

8. **Brain-Controlled Wheelchair (2006)**

   Rebsamen et al., 2006 [34] presented the first working prototype of a brain-controlled wheelchair, the ideal model for people who are not able to use other interfaces, such as a hand joystick. This equipment was capable to navigate inside a typical office or hospital environment. It relies on a path following strategy that provides simple control of necessary movements and it used information from EEG signals, more specifically the single display paradigm P300 system [35], to generate simple commands.

9. **RoboChair(2009)**

   Later in 2009, from the need of a reusable framework for software and hardware developments of navigation applications, came up the RoboChair. Thus, the robotic wheelchair is an open framework for assistive applications, design modular and based on standard interaction devices as a joystick and touch screen, for easy extension, interoperability and low cost [14, 36].

10. **Intellwheels 1.0 (2007) & Intellwheels 2.0 (2015)**

    The Intellwheels Project arose in 2007 at the Artificial Intelligence and Computer Science Laboratory (LIACC) of the University of Porto in consortium with other R&D institutions, more specifically, INESC TEC, and the University of Aveiro. In this first edition a simple IW prototype was developed [37], where typical capabilities of this system were tested, including: voice and sensor control, facial expressions recognition, advanced sensory capabilities, obstacle avoidance, intelligent task planning and also communication with other devices [20, 26, 38, 39].

    The second iteration of this project, Intellwheels 2.0, appeared to follow up the previous project. It will pretend to consolidate the respective innovative ideas and developing four fully functional products: IW Framework/kit, which allows to transform different types of commercial wheelchairs into IWs; Realistic IW simulator, with 3D interface, virtual reality and containing three serious games to learn and train the IW driving; Flexible and Complete Multimodal Interface capable to cooperate with several other intelligent devices; Complete IW prototypes using the framework/kit and multimodal interface developed [20].

    Therefore, this project aims to create a wide range of prototypes and products, functional and innovative, that will increase the autonomy and improve life quality of disabled people.

It should be noted that the future work to be performed during the thesis will contribute to this second phase of the project.

11. **The Wheelie (2017)**

    The first AI powered wheelchair, Wheelie, appears in 2017 at the HOOBOX Robotics startup [40]. This prototype uses facial expressions to control a commercial wheelchair. Although some previous solutions have been developed with the same goal [41], these have not achieved a satisfactory performance.

    Wheelie through a 3D camera with Intel RealSenseTM technology recognizes eighty points around the face, eyes, nose, and mouth, and identifies nine facial expressions, converting them into wheelchair commands [21].

12. **Devigne et al. Wheelchair (2020)**

    Devigne et al., 2020 [22] proposed the first power wheelchair navigation assistance system using a wearable tactile solution. This solution was conceived mainly to improve navigation for people with visual and/or cognitive impairments.

    Through the use of one or two vibrotactile armbands, users obtain guidance feedback on the path to follow or the presence of obstacles. Despite receiving this vibrotactile stimuli, users are in charge of controlling the wheelchair. This enables them to move or deviate from the indicated trajectory.

2.3 Conclusion

ATs constitute fundamental and essential tools for the daily routines of a considerable part of society. They can strongly improve the independence and autonomy of their users, leading to more confident people.

By studying different types of people with low capacities or cognitive limitations and their needs, it is easy to realize that their mobility can be extremely dependent on a wheelchair. For this reason and with the great technological revolution of recent times new concepts have appeared, as for instance, the IWs. Within this concept, several prototypes have been implemented, highlighting the diversity of available input interfaces, from joysticks to brain waves and facial expressions.

Even though many developments have already been made in this domain, there is still plenty of space for evolution to reach an ideal wheelchair prototype capable of fulfilling everyone's needs.

Chapter 3

Adaptive Sensors

Currently, a greater concern for building a more inclusive and adapted future has been noted. Therefore different types of adaptive sensors should be studied. In this chapter, the concept of adaptive sensors will be first introduced (Section 3.1) and after that, two types of these sensors will be carefully discussed, Sensors for Hand Gesture Detection (Section 3.2) and EEG Sensors (Section 3.3).

3.1 Adaptive Sensors Concept

Over time and with the trend towards a smart society, humans are experiencing a growing connection to electronics in the digital world, which can greatly enhance our life and productivity [42].

Communication between human beings and machines, specifically computers, has been facilitated by the newest innovations in electronics and wearable technologies. This Human Machine Interface (HMI) system will be increasingly relevant to the Internet of Things (IoT) and universal computing [43]. Commonly, communication begins when an object/machine, collects and interprets a human's desire. Therefore, for the HMI, is essential an input device, for example an adaptive sensor, which can capture the user's intention [44].

Considering the attractive properties of sensors for detecting Hand Gestures and EEG sensors, these will be the two groups of sensors thoroughly studied in the following Section.

3.2 Sensors for Hand Gesture Detection

Presently, million of people in the world are suffering from paralysis, so new forms of interaction with HMI must be explored. Thereupon, human hand gestures have shown an important role of real-time input for devices offering an HMI.

3.2.1 Hand Gestures

The language of the human body plays an essential role in communication, it is useful to transmit, exchange, interpret and understand people's thoughts, intentions, or even emotions [44]. Body language not only supports or emphasizes spoken language but is also a fully functional language in itself.

According to Mitra et al., 2007 [45], gestures could be categorized taking into account the association with speech, linguistic properties, spontaneity and social interaction. This proposed list is comprised of:

1. ***Gesticulation*** - It constitutes about 90% of human gestures and corresponds to voluntary movements of arms and hands. Blind people also often gesticulate when talking to each other;

2. ***Languagelike gestures*** - gesticulation included into an oral communication, replacing a certain spoken word or sentence;

3. ***Pantomimes*** - gestures describing objects or actions, which could or could not be supported by speech;

4. ***Emblems*** - popular signs, for example "V for victory";

5. ***Sign languages*** - highly structural language.

The previously described list has been organised so that as the list progresses, the association with speech decreases, language properties rise, spontaneity declined, and social regulation increases.

Therefore, hand-pose is considered as one of the most important communication tools in daily life. Adding this to the growing advance in image and video processing techniques has led to new investigations into human-machine interaction incorporating gesture recognition. Subsequently, a wide range of possible applications was identified [45, 46], in particular in the domain of Virtual Reality, Robotics and Tele-presence, Games and Desktop/Tablet PC Applications. As a consequence, human gestures provide an ergonomic and interesting approach to entry to the HMI.

3.2.2 State of the Art

The recognition of hand gestures consists not only in following the human movement, but also in interpreting that movement as semantically significant commands [47]. Consequently, gesture recognition research intends to develop systems capable of identifying specific gestures and using them to communicate or control a device. However, gestures need to be segmented in spatial and temporal domains for the right interpretation of human's intention [48]. The static structure of the hand contains information about the hand posture, while the dynamic part corresponds to the gestures.

For this gesture detection, two techniques are commonly used: Data Gloves or Vision based methods [47] (Figure 3.1). The first method determines the hand posture through sensors (mechanical or optical) attached to a glove, which allow the conversion of finger flexions into electrical signals. A method that requires several cables connected between the computer and user, hindering the spontaneity of interaction. The second one, computer vision based technique, is non-invasive and based on the way human beings understand information from their surroundings.

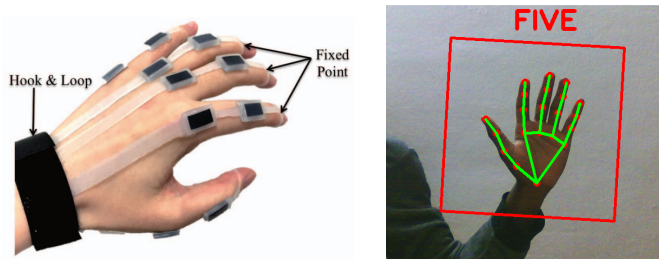

(a) (b)

Figure 3.1: Hand Gesture Recognition approaches: (a) Data Glove Method (adapted from [49]); (b) Vision Based Method (adapted from [50]).

In order to perform more human-like interfaces between humans and machines, an efficient and real time gesture recognition must be ensured [51]. According to this, Murthy et al., 2009 [47], enumerated some requirements for a successful vision based system, namely:

- **Robustness:** The system should be user independent and sufficiently robust against noise and incomplete visual information;
- **Computational Efficiency:** The vision and learning algorithms should be effective as well as cost efficient;
- **Scalability:** The system should be able to easily adapt to different applications;
- **User's Tolerance:** Malfunctions or failures in interaction should be tolerated. A repetition of an action is preferable to a wrong decision by the computer.

Considering all the features mentioned above, four devices for hand gesture and motion tracking could be distinguished (Figure 3.2): Microsoft Kinect, Intel RealSense Depth Camera, Microchip's MGC3X30 and Leap Motion [56].

The Microsoft Kinect is a body tracking device used for games and real-world applications as diverse as digital signage, virtual shopping, education and telehealth [52, 57].

The Intel RealSense Depth Camera has the ability to calculate depth and enable devices to see, understand, interact with, and learn from their environment [53]. It allows not only face tracking and recognition capabilities, but also hand motion tracking.

Microchip's MGC3X30 are controller chips based on GestIC® technology which recognize 3D gestures and track motion [58]. This technology uses an electric field (E-field) for advanced

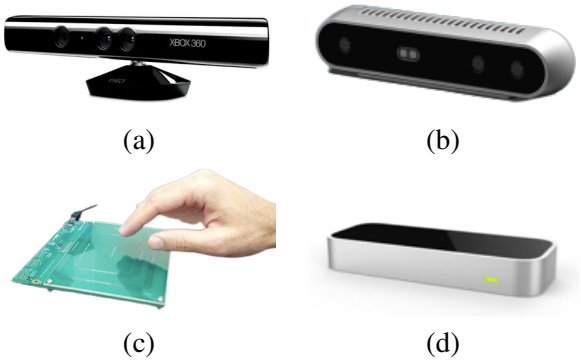

(a) (b) (c) (d)

Figure 3.2: Devices for hand gesture and motion tracking: (a) Microsoft Kinect (adapted from [52]); (b) Intel RealSense Depth Camera (adapted from [53]); (c) Microchip's MGC3X30 (adapted from [54]); (d) Leap Motion (adapted from [55]).

proximity sensing that can detect, track and classify a user's hand or finger motion in free space [59].

The Leap Motion is an optical hand tracking Controller that captures hand movements with outstanding accuracy [55].

A comparison between the main features of these devices is shown in Table 3.1.

Table 3.1: Comparison of hand gesture and motion tracking devices (adapted from [56]).

Device	**Microsoft Kinect**	**Intel RealSense Depth Camera**	**Microchip's MGC3X30**	**Leap Motion**
Applications	- Xbox gaming; - Robotics;	- Desktop applications; - Robotics; - Augmented and Virtual Reality.	- Home Automation; - Industrial and Medical switches; - Game controllers.	- Desktop applications; - Touchless public interfaces.
Advantages	- Good depth sensing with a clean depth image; - Skeleton tracking: up to 6 skeletons and 25 joints/skeleton.	- Good construction quality and very sturdy; - Operates both inside and outside; - Built for close range tracking and has incorporated gesture recognition such as "grab and release".	- No host processing required; - Includes a powerful on-chip gesture library.	- Robust and reliable skeletal mode - Very fast and accurate finger tracking.
Limitations	- Hands and fingers cannot be easily distinguished; - Difficulty in recognizing small gestures.	- The overall level of noise is relatively high; - Sometimes reveals problems in capturing small geometric details.	-	- Decreases its performance when operated in sunlight; - Reduces recognition capacity when two fingers are in contact.
Price	$150.00	$189.00	$172.81	$88.95

As already stated, human hand gestures and motion tracking could be an interesting approach to facilitate daily routines, hence the importance of an analysis of the relevant work already done on this topic (Table 3.2).

Table 3.2: Summary of related works regarding sensor-based gesture recognition.

Reference	Used Sensor(s)	Description
Van den Bergh et al., 2011 [60]	Kinect	System for the navigation of robots inside buildings based on hand gestures recognition
Montanaro et al., 2016 [61]	MGC3130 and Leap Motion	Touchless interface based on gesture recognition for the control of an elevator
Chaitanya et al., 2017[62]	MGC3130	Handling household appliances through hand gestures (e.g. TV and radio)
Park et al., 2017 [63]	Kinect	Effects of Virtual Reality Training using Xbox Kinect on Motor Function in Stroke Survivors
Liao et al., 2018 [64]	Intel RealSense Depth Camera	Static hand gesture recognition system with a depth camera, a promising work for dynamic real-time sign language recognition
Zhao et al., 2018[65]	Leap Motion	Hand gesture recognition for remote control of a drone
Feng et al., 2020 [66]	Kinect and Leap Motion	Comparison of Kinect and Leap Motion for Intraoperative Image Interaction
Fereidouni et al., 2020 [67]	Leap Motion	A novel design and implementation of wheelchair navigation system using Leap Motion sensor

3.2.3 Leap Motion

As previously mentioned, Leap Motion Controller is an optical sensor capable of detecting and tracking hand movements. This controller simplifies the interaction with digital content, making it more authentic and effortless.

Since Leap Motion is the sensor used in future work, its architecture and Application Programming Interface (API) will be analysed in detail in the next subsections.

3.2.3.1 Hardware

Leap Motion is a small device, as shown in Figure 3.3, with an aluminium and scratch-resistant glass construction created by Ultraleap.

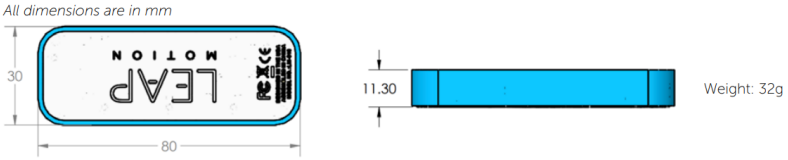

Figure 3.3: Leap Motion Dimensions (adapted from [68]).

Regarding its components, two cameras and three LEDs can be mentioned (Figure 3.4). The two 640x240-pixel near-infrared cameras are spaced 40 millimeters apart and operate in the 850-nanometer spectral range. Due to the large angles of the camera lenses, the sensor has a wide area of interaction. This interactive zone could be described as an upside-down pyramid with a depth between 10cm to 60cm preferred, up to 80cm maximum, directly above the controller device. It should be noted that the range is limited by the propagation of LED light through space [68].

The LEDs are spaced on both sides and between the cameras to avoid overlaps. These detect infrared light with a wavelength of 850 nanometers, which is outside the visible light spectrum [69].

Figure 3.4: Leap Motion Structure (adapted from [68]).

Once purchased, the package includes the Leap Motion Controller, a quick setup guide and an USB 2/3 hybrid cable.

3.2.3.2 API Overview

The Leap Motion system is configured assuming a right-handed Cartesian coordinate system with the origin centered on the top of the device. The configuration of the x-, y- and z-axes could be observed in Figure 3.5. Just note that the positive direction of z-axes matches to the user's direction.

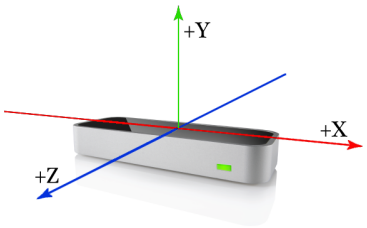

Figure 3.5: Leap Motion Coordinate System (adapted from [69]).

Concerning the measurement units, Leap Motion API evaluates the distance in millimeters, the time in microseconds, the speed in millimeters/second and the angles in radians.

The device could track hands, fingers, and tools within its field of vision. The results of the tracked entities could be found in a frame of data that contains information related to the overall motion detected. For calculating these motions, data from two frames are required. As result, different types of motions could be detected, particularly Scale (e.g., one hand moves closer to the other), Rotation (e.g., change of the orientation of the hand) and Translation (e.g., move hands to the left) [70]. Besides that, the list of fingers and/or tools associated with the detected hand could also be provided. The classification in tools or fingers depends on their shape because a tool is usually longer, thinner, and straighter than a finger. For both situations, the position and direction vectors are given to the user.

In addition, the Leap Motion Software could identify some movement patterns as gestures which are also reported in a frame. The four gestures recognized (Swipe, Circle, Key Tap, and Screen Tap) are schematized in Figure 3.6.

The full information about the API Overview could be found in the Leap Motion Developer Portal – API Overview [69].

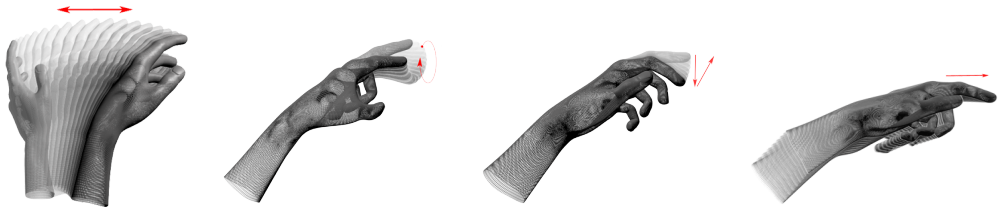

(a) (b) (c) (d)

Figure 3.6: Gestures recognized by the Leap Motion software (adapted from [69])): (a) Swipe; (b) Circle; (c) Key Tap; (d) Screen Tap.

3.2.3.3 System Architecture

The Controller supports the most common operating systems, Windows, Linux, and MAC. It is connected to other devices through an USB cable included in the package. In order to get tracking data, the Leap Motion Software Development Kit (SDK) provides two varieties of APIs:

- **Native Interface**: used to create new Leap-enabled applications. It is accessible from a dynamically loaded library that connects to the Leap Motion Service. The library could be directly linked into C++ and Objective-C applications, or through one of the language bindings available for Java, C#, and Python;
- **WebSocket Interface**: when combined with the JavaScript client library, it allows the development of Leap-enabled web applications.

The full information about the Leap Motion architecture could be found in Leap Motion Developer Portal – System Architecture [71].

3.3 EEG Sensors

Electroencephalography (EEG) sensors are responsible for monitoring the electrical signals of the brain. These electronic devices measure the variable electrical signals produced by the activity of large groups of neurons near the surface of the brain for a certain period of time [72].

Typically, these sensors are used in Brain-Computer Interfaces (BCI), also known as Brain–Machine Interfaces (BMI). BCIs enable the control and steering of mechanical and/or electronic equipments by collecting and processing EEG data in real time [73, 74].

3.3.1 Electroencephalography

Electroencephalography is an electrophysiological procedure to record electrical activity originating in the human brain [75]. Its first recording was of the responsibility of a German psychiatrist, Hans Berger, in 1924.

From the perspective of electroencephalogram acquisition, two techniques could be employed - invasive or non-invasive. The invasive method requires electrodes surgically implanted at the surface or depth of the brain. Due to its level of invasiveness and specificity, signal quality, in terms of distortion and amplitude, is better; nevertheless, a surgical procedure is mandatory [76]. The non-invasive technique measures the activity through a set of electrodes placed on the subject's scalp.

Both approaches incorporate various types of artefacts derived from internal and/or external sources which explain the need for pre-processing of these signals. Internal source artefacts are associated with the subject's physiological activities, namely electrocardiography (ECG), electromyography (EMG) and electrooculography (EOG). External source artifacts are all those arising from environmental interference, recording equipment, and cable movement [77, 78].

3.3.1.1 Brain Activity Patterns

The brain, one of the most complex body organs, can be divided into three regions: brain, cerebellum, and brain stem. Moreover, the brain comprises two cerebral hemispheres, the outer layer - cortex (grey matter), and the inner layer (white matter) [79].

Taking into account that the cortex is the largest portion of the brain, its structure also has to be stated. The cortex consists of four lobes, frontal, temporal, parietal, and occipital, each of them having a specific function assigned [77, 80]:

- **Frontal:** essential for cognitive functions and control of voluntary movements;
- **Temporal:** related to sound processing;
- **Parietal:** involved in receiving contralateral sensory information;
- **Occipital:** receiving and recognizing visual stimuli.

Depending on the stage of the brain activity, particularly wakefulness, coma, or sleep stages, when EEG data is analysed different types of neural oscillations (or brain waves) could be categorized [81]. Thus, this classification is based on brain signals frequency and location. According to these features, the main brain waves are described in Table 3.3 and represented in Figure 3.7.

The greater the knowledge and understanding about these waves, the different processing can be done, increasing their range of applications.

Table 3.3: Brainwaves related to different EEG frequencies (adapted from [77, 81, 82]).

Band	Frequency (Hz)	Cortex Lobe	Characteristics
Delta	0.5 - 3.5	Throughout the cortex	Dominant in dreamless sleep and in deep meditation state
Theta	3.5 - 7.5	Parietal and Temporal	Associated with access to unconscious material, creative inspiration and deep meditation
Alpha	7.5 - 12	Occipital	Dominant in the resting state, Mental coordination and Calmness;
Beta	12 - 30	Frontal and Parietal	Related to focused concentration, cognitive tasks and decision making
Gamma	> 30	Somatosensory cortex (Parietal Lobe)	Reflects the mechanism of consciousness

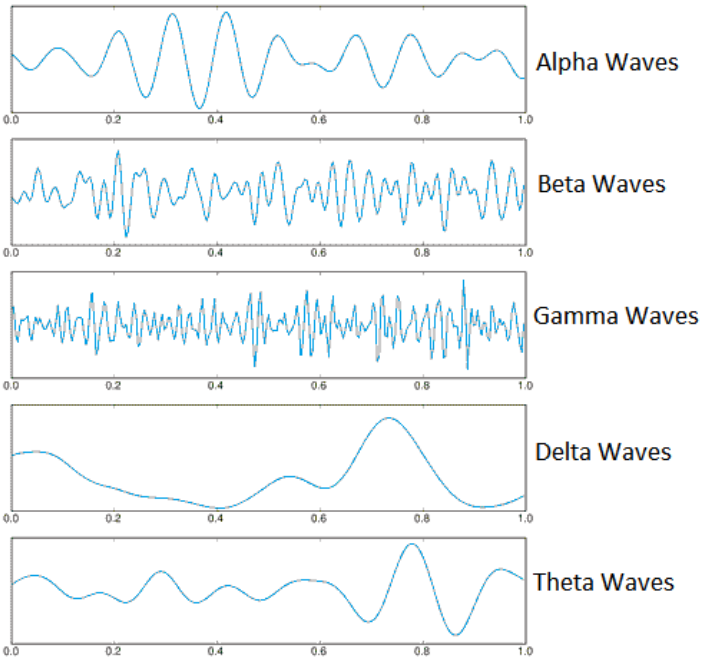

Figure 3.7: Representation of the main human brain waves (from [81]).

3.3.1.2 Interpreting brain activity - Neuro-mechanisms

Once the brain activity in different portions of the brain is studied, different neuro-mechanisms are identified. These signs, described by neuro-mechanisms, are fundamental to control a BCI. Thereupon, a neuro-mechanism that encompasses as many changes in brain activity as possible during an event, represents the best option [77].

The most common families of neuro-mechanisms used for attributing a signal to an event or intention in a Brain-Computer Interface are summarized below.

1. **Sensorimotor Activity**

   In the absence of external or internal intervention, the brain has a continuous (rhythmic) action. During an event, these rhythms can fluctuate, resulting in two neuro-mechanisms: Event-Related Desynchronization (ERD) and Event-Related Synchronization (ERS). These can suppress or improve rhythmic brain activities, respectively. Hence, by interpreting the amplitude of the signal at certain frequencies acquired from specific locations in the brain, it is possible to conclude about the underlying brain activity [83].

2. **Event-Related Potentials (ERP)**

   ERP are small amplitude deviations in the brain signal, timestamped to an event [77]. Typically, the triggering event, direction of deflection, observed location and latency are indicators of these potentials [83]. Their detection can reveal a person's reaction or intention.

3. **Steady-State Evoked Potential (SSEP)**

   After a brain stimulus is applied, it has a particular frequency and is processed in a specific brain region. Once processed, its amplitude is proportionally improved relatively to the stimulus frequency [77]. This phenomenon is called SSEP and can be used to determine which stimulus the person was observing attentively. From this neuro-mechanism, a subtype named Steady-State Visually Evoked Potential (SSVEP) is identified for visual stimuli. In this one the enhancement occurs in the occipital cortex [83].

3.3.2 State of the Art

BCIs could be considered as a communication system to convert humans' mind or will into commands to manipulate devices. Consequently, these interfaces are immensely helpful to support people with motor disabilities or completely paralyzed people, since the communication has a direct pathway between brain and external devices [84].

Currently, BCIs have an extensive range of applications, from rehabilitation engineering, intelligent assistive robot to non-medical fields, for instance gaming and biometric identification. That is why, they are getting popularity among the researchers [85].

In accordance with Soufineyestani et al., 2020 [73], these applications can be separated into 3 domains, as can be seen in Table 3.4.

Table 3.4: BCI applications (adapted from [73]).

Category	Application	Reference
Autonomous navigation of digital or mechanic devices	Real-time teleoperation of robotic body parts	[86–89]
	Controlling and directing a robot, drone, dashborad of a vehicle, or a miniature or semi-automated car	[90–93]
	Monitoring and controlling sensors inside of smart houses	[94]
Helping people with disabilities or motor activity impairment	Control of mobile phone apps using eyewinks	[95]
	Directing electrical wheelchair movement	[96–99]
	Control of artificial body part (e.g., prosthetic hand or arm)	[100, 101]
	Post-stroke motor rehabilitation	[102]
	Mind-controlled dialing systems	[103]
	Communication system for people with speech disability	[104]
	Mouse cursor control using imagined hand movement	[105]
	Gaze controller for patients with neurodegenerative diseases	[106]
Neurogaming and Entertainment	Controlling a video game or virtual reality environment using eye movement	[107]
	Control of fibre optic clothing	[108]

For the purpose of providing a BCI, a presence of a device is imperative to collect information about brain activity. Several options for EEG devices are available on the market. However, the Neurosky MindWave Mobile 2, Muse 2, Ultracortex Mark IV, and the Emotiv Epoc (Figure 3.8) are highlighted for being non-invasive EEG headsets, and for measuring multiple parameters [109]. These properties make their use more convenient and comfortable for operators. Table 3.5 compares these EEG Headsets.

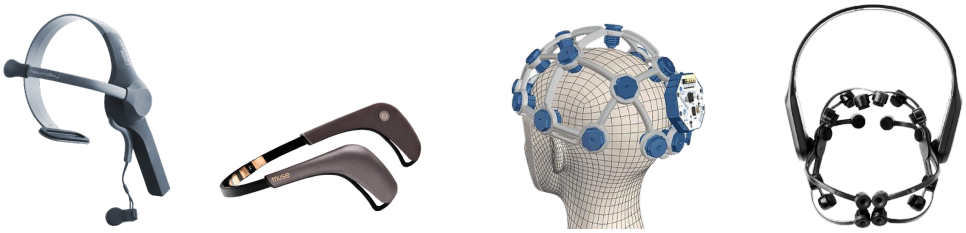

(a) (b) (c) (d)

Figure 3.8: EEG Headsets: (a) NeuroSky MindWave Mobile 2 (adapted from [110]); (b) Muse 2 (adapted from [111]) ; (c) Ultracortex Mark IV (adapted from [112]); (d) Emotiv EPOC X (adapted from [113]).

The NeuroSky MindWave is a single-channel, dry EEG headset that measures and transmits data via Bluetooth Low Energy or classic Bluetooth [110].

Muse 2 is a brain sensing headband that offers measurements of EEG and photoplethysmography (PPG) and provides instant feedback of brain activity [111].

The Ultracortex Mark IV is an open-source, 3D-printable headset designed to operate with any OpenBCI Board [112]. It can evaluate different parameters such as EEG, muscle activity, and

Table 3.5: Comparison of EEG Headsets (adapted from [109]).

Device	**NeuroSky MindWave Mobile 2**	**Muse 2**	**Ultracortex Mark IV**	**Emotiv EPOC X**
Sensors	- Ear-clip - Sensor Arm	- EEG brain sensors : 2 on the forehead, 2 behind the ears plus 3 reference sensors	- Wet electrodes	- Two Electrode Arms - 14 - Channel EEG (whole-brain sensing)
Features	- 8 hours of battery life - Supported platforms: Windows, Mac, iOS and Android	- 5 Hours of Continuous Use - Adjustable arms - A Muse application is available to track progress over time	- 3D-printable EEG headset - Sampling capacity of up to 16 EEG channels from up to 35 different 10-20 locations	- 9 hours of battery life - Rotating headband - Saline-Based Electrodes
Parameters Evaluated	- EEG power spectrums (Alpha, Beta, etc.) - Attention and Meditation levels - Eye blinks	- Mind (EEG) - Heart and Breath (PPG + Pulse Oximetry)	- EEG - EMG - ECG	- Mental Commands - Performance Metrics: Excitement, Engagement, Relaxation, Interest, Stress, Focus - Facial Expressions: Blink, Wink, Surprise, Smile, Clench, Laugh
Price	$109.99	$249.99	$299.99 - 849.99	$849.00

heart activity.

Emotiv EPOC X is an EEG headset that features two electrode arms allowing coverage of the temporal, parietal and occipital lobes [113].

3.3.3 NeuroSky MindWave Mobile 2

As already stated, NeuroSky MindWave Mobile 2 is a single-channel, affordable and dry EEG headset. It stands out for its simplicity and number of measured properties, in particular power spectrum (delta, theta, alpha, beta, and gamma) and attention and meditation levels. Additionally, this device offers raw brain waves with sampling rate of 512Hz [110].

3.3.3.1 Hardware

The MindWave device incorporates a T shaped headband, a wider ear clip, a flexible sensor, and an adjustable arm. The reference and ground electrodes are positioned on the ear, whereas the EEG electrode is on the sensor arm, this is, it is located on the forehead above the left eye [109]. For its functioning it is powered by a single AAA battery, which confers it an 8-hour autonomy.

Figure 3.9 illustrates a schematic representation of this headset.

Furthermore, it is user-friendly, ergonomic and designed to optimize comfort during usage. After a properly positioned and turning on the power switch, a luminous feedback can be seen. This light indicator is located near the power button and indicates the status of the device. The meanings of the LED indicator colours are specified in the Table 3.6.

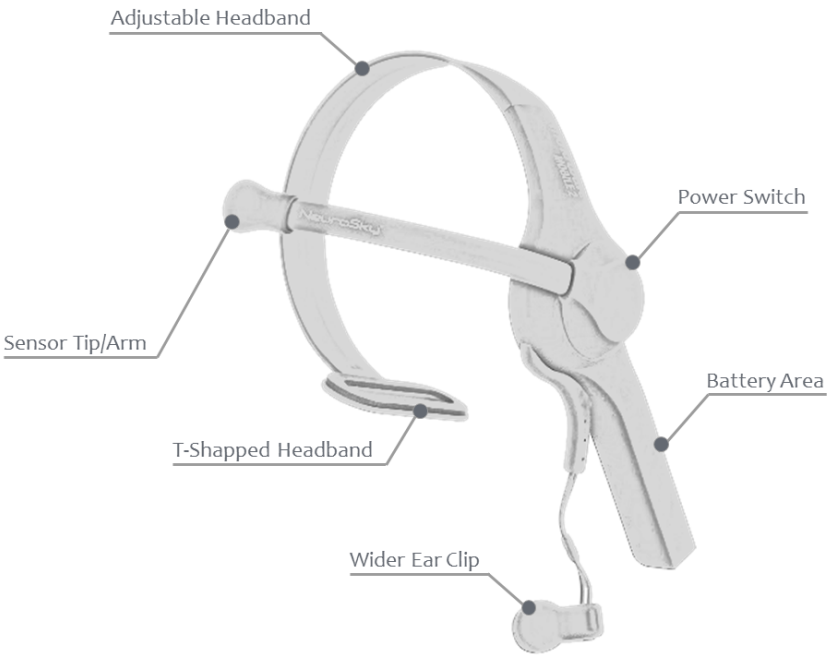

Figure 3.9: Schematic representation of NeuroSky MindWave Mobile 2.

Table 3.6: LED indications on NeuroSky MindWave Mobile 2 (from [114]).

Light	Headset State	Meaning
Off	Powered Off	Headset is turned off or has no battery
Solid Red	Low Battery	Headset needs a new battery
Solid Blue	Powered On	Headset is turned on

3.3.3.2 System Architecture

The headset could be connected to several platforms, with Windows, Mac, iOS and Android being examples. It transmits data wirelessly via bluetooth.

Many programming languages can be used for raw signal processing. In order to access headset functionalities from external software besides Neurosky, the ThinkGear Connector (TGC) was developed. TGC will allow the directing of headset data from the serial port to an open network socket, allowing communication through a library present in any language or framework [114].

3.4 Conclusion

Adaptive sensors are powerful tools to facilitate and simplify HMIs. Among the multiple existing sensor options, in this chapter the study was focused on hand movement recognition devices and sensors that enabling the analysis of brain activity.

Analysing the specificities of the wheelchair area and considering the future work, Leap Motion and Neurosky MindWave Mobile 2 demonstrated to be two interesting options for being incorporated in the interface of an IW. Giving this IW new possibilities to decode the user's intention. Leap Motion will be responsible for interpreting different commands given by hand movements. While NeuroSky through neuro-mechanisms will record users' desires, since the activity manifested in the various lobes can be described as signals which will be used to drive a BCI.

Chapter 4

Methodologies

Driving an IW requires several commands. In this study, the four basic commands, forward (Front), stop, go to the left and to the right will be assumed as the desired classes.

In summary, Leap Motion is an alternative to the conventional joystick wheelchair and through hand gestures will be able to interpret the user's intention. NeuroSky MindWave Mobile 2 is an EEG headset capable of recording brain waves. When a movement is imagined, even without being performed, it produces brain rhythms [115] . These types of imagination-based activities, commonly known as motor-imagery (MI), will be the ones used in this work.

The general approach followed for both sensors was based on the same principles, which means starting with data acquisition, then processing, feature extraction and lastly classification. However, this chapter presents two main sections one for each sensor, in order to facilitate the understanding of the methodology applied in each situation.

Additionally, it should be noted that all procedures were carried out in agreement with the ethical standards of the 1964 Helsinki declaration and an informed consent was filled out by each participant, an example of which is presented in Appendix A.

4.1 Leap Motion

4.1.1 Data set description

Based on Boyali et al., 2015 [116], four gestures were selected to achieve a wheelchair autonomous control (Figure 4.1). Therefore, this data set incorporates data from five different people, three of them aged between 20 and 24 years and the other two aged 52 years. This age difference and having three participants be female and two male greatly increased the variety and quality of data, given that the hand sizes were different.

The acquisition protocol is explained in the diagram presented in Figure 4.2. The first phase was preparation in which the volunteers were snugly seated in a chair placed in front of a computer. The next 4 seconds were the time to observe a visual cue, which represents the movement to be executed. After a sound was emitted, the subject performed the action, using the gesture shown in Figure 4.1. At last, the data recording was concluded with a beep.

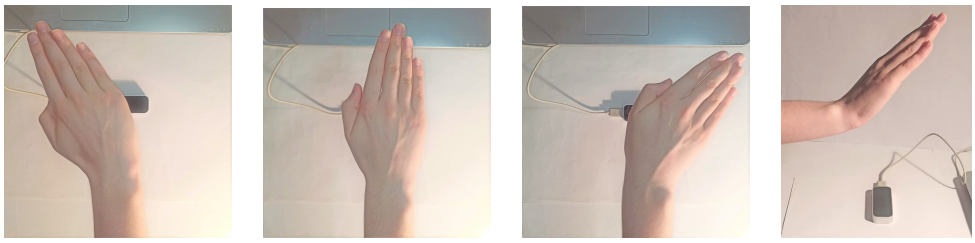

(a) (b) (c) (d)

Figure 4.1: Gestures representing the wheelchair steering commands: (a) Left; (b) Front; (c) Right; (d) Stop.

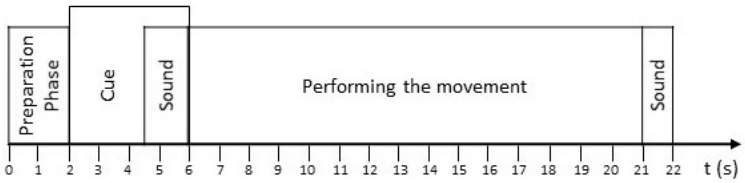

Figure 4.2: Timing schedule of the acquisition protocol for the hand gesture data set.

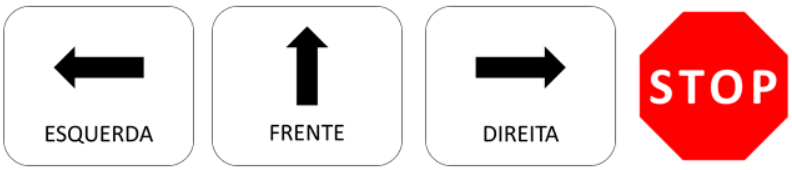

Figure 4.3: Example of the visual cues (from left to right corresponds to the classes Left, Front, Right and Stop).

To highlight, since all participants in the study are native Portuguese speakers, the visual cue is composed of an arrow accompanied by the respective direction written in Portuguese (Figure 4.3).

4.1.2 Data processing

4.1.2.1 Data Division

For each gesture, 1 500 samples were collected per participant. The data of all gestures were randomly organised and afterward partitioned into two parts, 80% for training and 20% for testing, which results in 24 000 and 6 000 respectively.

When analysing the data per subject, in total this translates into 4 800 for training and 1 200 for testing.

4.1.2.2 Feature Extraction

The Leap Motion device provides an extensive API where numerous parameters are available to use as features without requiring pre-processing. Taking into consideration the purpose of this work, the angles of yaw and pitch were chosen. These two variables were adopted as well by Boyaly et al., 2015 [116] and Mohandes et al., 2015 [117] in their studies on Gesture and Posture Recognition. Furthermore, the palm velocity was also included.

The detailed description of these features is given below.

1. **Yaw Angle**

   The yaw angle quantifies the rotation around y-axis (Figure 4.4), thus it is an important value to consider for horizontal hand movements, particularly for radial and ulnar deviation or, in other words, for left and right movements, respectively [118]; hence, for example, when subjects perform the movement to the right, it is expected an increase in this angle value to positive values, reaching the maximum values while the opposite behaviour should happen in movements to the left.

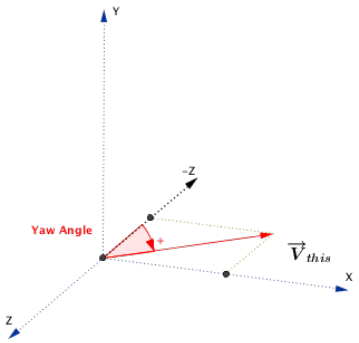

Figure 4.4: Representation of Yaw Angle (adapted from [68, 119]).

2. **Pitch Angle**

   The pitch angle evaluates the rotation around the x-axis (Figure 4.5), an interesting parameter for hand flexion and extension movements [118]. Looking at the gestures mentioned (Figure 4.1), the stop motion is associated to an extension of the wrist, making this value play an important role.

3. **Palm velocity**

   This parameter expresses the change rate of the palm position in millimeters/second [69] and it is subdivided into the velocities according to the x, y and z axes. Although the gestures used are static, certain people could have particular hand tremors that influence the classification. Therefore, this feature intends to capture data to avoid this problem.

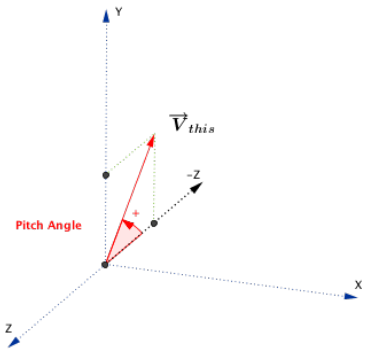

Figure 4.5: Representation of Pitch Angle (adapted from [68, 119]).

4.1.2.3 Feature Selection and Dimensionality Reduction

Feature selection and Dimensionality reduction are two crucial points that contribute to the achievement of better outcomes. The first concept corresponds to the identification of the most relevant features for the classification problem. While the second, dimensionality reduction, is defined by Van Der Maaten et al., 2009 [120] as the conversion of high dimensional data into a significant representation of reduced dimensionality. Succinctly, this technique provides a possibility to represent the relevant information from the data by requiring less information to do so.

Regarding feature selection, due to this being a classification task and the input data being numerical, the ANOVA F test was chosen. This method estimates the F distribution through the relationship between the group variance and within-group variance [121]. Subsequently, the significance level, p, is analysed and when lower than 5% indicates that the feature is statistically significant.

For dimensionality reduction, Principal Component Analysis (PCA) was the approach used, since it demonstrates to be a method, which despite being traditional, offers optimal results [120]. PCA aims to transform data by projecting it into a new orthogonal coordinate system based on an eigenanalysis of the data [122].

It should be highlighted that before dimensionality reduction, two feature scaling techniques, normalization and standardization, were tested to understand which one was more suitable.

4.1.2.4 Classification

The classification aims to discriminate four classes (Front, Stop, Left and Right) for that several classifiers and combinations of classifiers were implemented. In order to evaluate the performance of each predictive model created, two metrics were studied - F1-Score and Confusion Matrix.

F1-Score is a statistical measure based on the harmonic mean between precision (proportion of positive cases that were correctly identified) and recall (proportion of actual positives was identified correctly) [123].

The confusion matrix is represented as an $N \, x \, N$ table, where N is the number of classes. The columns contain information about the predicted classifications and the rows are the actual classes

[124]. Thus, this matrix gathers insights related to true positive (TP) or negative (TN) instances and also, false positives (FP) and negatives (FN).

Concerning the classifiers, linear and non-linear classifiers were trained, among which:

1. **Gaussian Naïve Bayes (GNB)**

   Naïve Bayes methods make predictions based on prior knowledge and current evidence [125]. In essence, the assigned class is the one to which the probability of belonging is greatest.

   The assumption of the probability distribution of features differs across the several Naïve Bayes classifiers. In this case, GNB, it is assumed to present a Gaussian distribution.

   The functioning of this classifier can be seen in Figure 4.6. For each data point, the z-score distance from that point to each class mean is computed, specifically the distance from the class mean divided by the standard deviation of that class [126].

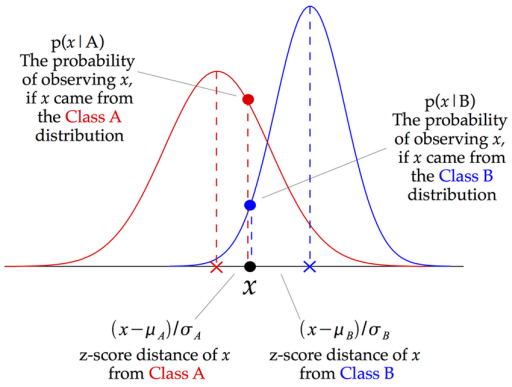

Figure 4.6: Illustration of how a GNB classifier works (adapted from [126]).

2. **K-Nearest Neighbours (K-NN)**

   A K-NN algorithm is a data classification technique that estimates the probability of a data point be a member of one group or another, depending on which group the closest data points are in. Therefore, it is a non-parametric learning method, or in other words a lazy learner, it does not build a model using the training set until a query of the data set is performed [127].

3. **Linear Discriminant Analysis (LDA)**

   LDA assumes that all classes are linearly separable and accordingly to this designs a hyperplane where the features are projected. This hyperplane is created by maximizing the distance between the mean value of these classes, and minimizing the variance within each category [128].

4. **Decision Tree (DT)**

   A decision tree is a flowchart-like structure where an inner node represents a feature (or attribute) extracted from the object, the branch represents a decision rule, and each leaf node the corresponding class, as can be observed in Figure 4.7 [129].

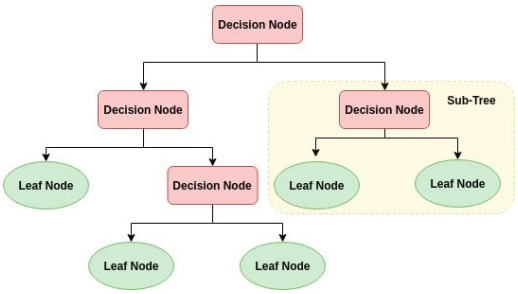

Figure 4.7: Architecture of a Decision Tree (adapted from [129]).

5. **Random Forest (RF)**

   Random forest is a tree-based method. It builds several trees, giving a prediction for each one. In the end, the predicted class is the result of the main vote between the different trees [130]. Trees can be considered weak predictors, but in the total ensemble they could make good predictions.

6. **Logistic Regression (LR)**

   This method is a supervised learning algorithm that estimates the class of an object based on a linear combination of the objects' features, as described in Equation 4.1, in which x corresponds to the features and θ to the coefficients [77]. The best model arises from minimizing the difference between the model prediction and the true values, i.e., the loss function.

$$f_\theta(x) = \theta_0 x_0 + \theta_1 x_1 + \ldots + \theta_n x_n = \theta^T x \tag{4.1}$$

7. **Support Vector Machine (SVM)**

   This model consists of representing the multiple classes into a hyperplane in multidimensional space. This hyperplane derives from an iterative process whereby the error can be minimized [131]. The final purpose is to distribute the data sets into classes that maximise the margin of the hyperplane (Figure 4.8).

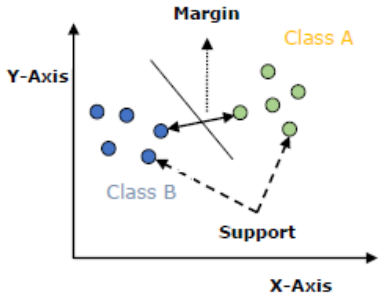

Figure 4.8: Representation of the SVM classifier in a 2-dimensional example (adapted from [131]).

The SVM classifier can perform linear and non-linear classification. In the first possibility, Linear SVM (LSVM) splits the data with a hyperplane, drawing a straight line. Meanwhile,

for non-linear classifications, the data sets are mapped by kernel functions into higher dimensionality spaces, to enable their separability.

8. **Multilayer Perceptron (MLP)**

   MLP is a neural network where the input units and the output layer are fully connected by hidden intermediate layers. Each node, except the input nodes, has a non-linear activation function where a weight is assigned to each feature [132]. For training, this classifier adopts a supervised learning technique named backpropagation, which means that it continuously adjusts the weights of the connections in the network in order to minimise the difference between the actual output vector of the network and the targeted output vector [133].

After all the explained classifiers were tested, **Voting and Boosting** techniques were also implemented. These new approaches are Ensemble methods designed to create a stronger model by combining different predictions.

Voting classifiers combine predictions of multiple models, typically of different types, and the final results come from a majority vote [134]. Consequently, the final predicted class could be either the class that the majority of classifiers predicted or the averaged probability of belonging to the class, leading to **hard and soft voting**, respectively.

AdaBoost (Adaptive Boosting) trains and implements trees in sequence. Initially, it assumes several classifiers (weak learners) and combines their individual predictions [135]. After an iterative process, the weight assigned to each sample is modified, with incorrect classifications having a higher weight than correct ones. In this manner, the classifier tries to improve the misclassified samples by focusing on the higher weights.

Furthermore, during this training process the hyper-parameters of the classifiers were optimised. For this purpose, a grid search with a 10-fold cross-validation was applied.

4.1.3 Application

A real-time testing represents an essential step to evaluate if the proposed method operates as expected. According to this, two approaches were considered: an implementation of the developed models in the Intellwheels project's wheelchair simulator or the creation of a simple application with the main goal of controlling a robot/object that could symbolize a wheelchair.

Comparing both approaches, the choice fell on the second one. The integration of the work in the project simulator would be a long and time-consuming process since it implied the joining of several programming languages. Considering the available time, this process was not feasible and therefore, the second method was selected.

In conclusion, the proof of concept involved developing an application similar to a game in which a patient was supposed to drive a robot along a defined path where the four classes studied were present.

4.2 NeuroSky Mindwave Mobile 2

Considering this type of sensor, only data from one data channel is collected. For this reason, it is important to record data when subjects perform different tasks to understand the approach that leads to better results. In this context, four data sets were created, each one acquired under a specific condition, as described in the following section.

4.2.1 Data sets description

4.2.1.1 Data set A

Based on the acquisition protocol of BCI Competition 2008 (IV) Graz data set B [136], this data set consists of imagining one of four directions (front, left, right or stop) after the respective cue be displayed on the screen.

This data set includes EEG data of twelve different healthy subjects, all right-handed and with ages ranging from 20 to 24 years. Participants were seated comfortably in a chair, observing a flat screen monitor situated about 1 meter away at eye level.

Each experimental trial was approximately 22 seconds long per direction, as shown in Figure 4.9. The first 2 seconds correspond to a preparation phase in which the subject is adjusting the sensor to his head. After that, a visual cue (Figure 4.3) is presented for 4 seconds on the screen, followed by the 16 seconds of the imaginary period. In order to restrict and indicate the imagination period, there is also an acoustic sound at the beginning and at the end of this phase.

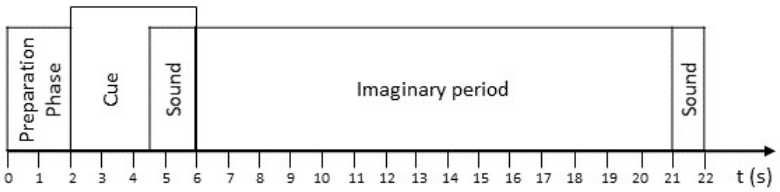

Figure 4.9: Timing schedule of the acquisition protocol for Data set A

4.2.1.2 Data set B & Data set C

Data sets B and C were created to investigate how a different visual stimulus could lead to an improved performance in wheelchair driving. According to this and motivated by Turnip et al., 2016 [137] work, participants were asked to imagine the wheelchair moving in a direction while watching that respective direction on a video format stimulus. For an easy and fast identification of which direction they should imagine at each moment of the video, it contained an arrow with the corresponding movement, as can be seen in Figure 4.10.

For data set B, this video involves a wheelchair simulator, while in data set C the video represents a roller coaster ride, a stronger stimulus.

(a) (b)

Figure 4.10: Example of a frame from the video stimulus used for the acquisition of: (a) Data set B; (b) Data set C.

Regarding the Acquisition Protocol (Figure 4.11), it started with a preparation phase, similar to data set A, followed by a warning sound and, after that, a 2-minute video was exhibited. Each video included three simulations per direction, being randomly alternated between them and having a duration of approximately 10 seconds each. Lastly, a sound was emitted to signaling the end of the data collection.

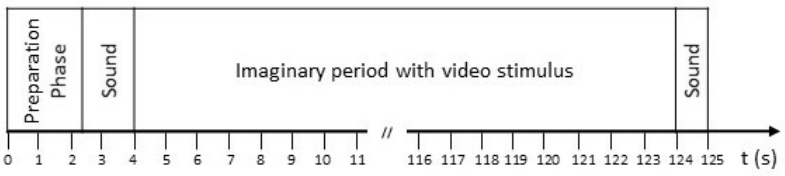

Figure 4.11: Timing schedule of the acquisition protocol for Data sets B and C.

This experimental acquisition comprises EEG data from the same twelve subjects described in data set A.

4.2.1.3 Data set D

These data arise to study the different classification classes through EEG data collected while participants drive a wheelchair on a predefined route (Figure 4.12).

For this acquisition, volunteers were first asked to fit the sensor and minimise their head movements. Next, a brief explanation was given on how to drive the wheelchair used, the one from the Intellwheels project, as well as the path to follow. All participants performed the route once for familiarization and training, and only then performed two repetitions of the route where EEG was recorded.

Ten participants took part in this test, all of them healthy and without previous experience in driving a wheelchair.

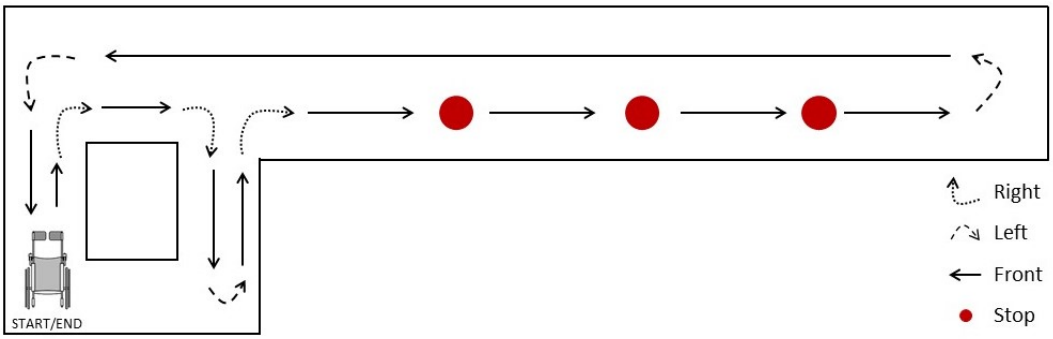

Figure 4.12: Top view of the route used for Data set D acquisition.

4.2.2 Data processing

4.2.2.1 Data Division

Similar to the split carried out on the Leap Motion data set (Section 4.1.2.1), in this analysis all data sets (from A to D) follow the same structure of 80% for training and 20% for testing.

In addition, to increase the number of data and taking into account that classification is sensitive to epoch length [115, 138], each extracted EEG signal was divided into non-overlapping segments with different time windows, 2, 3 and 4 seconds.

4.2.2.2 Pre-processing

After epoching the EEG data to the desired time windows, a resampling was required to ensure that all data had the same sampling rate [139].

Next, the EEG signal is recognised to have a significant amount of noise and ocular artefacts typically present at low and high frequencies. Hence, a bandpass filter, more specifically a Butterworth filter, was applied to remove all this noise. Finally, the signal comprises only the bands of interest, alpha and beta, in which the features will be extracted.

4.2.2.3 Feature Extraction

Obtaining features that could efficiently associate the EEG segments to the respective thought direction is the main goal of the feature extraction step. For this reason, features are extracted from several domains, namely time domain (Statistical and Fractal Dimension (FD) features), frequency domain (Power features) and time-frequency domain (Empirical Mode Decomposition (EMD) and Entropy features). All the extracted features, which are further described below, have been widely used for EEG-based MI recognition [140–144].

1. **Statistical Features**

   In order to characterise the time series of EEG signals six features were extracted, which are adapted from [145, 146].

- Mean
- Standard Deviation
- Mean Absolute deviation
- Hjorth Parameters:

  These parameters contain not only information about the frequency spectrum of a signal, but also enable, with low computational complexity, an analysis in the time domain. They are divided into 3 parameters, i.e. activity, mobility and complexity. The first, activity, represents the surface of the power spectrum in the frequency domain. The second corresponds to the calculation of the square root of the ratio between the variance of the first derivative of the signal and the signal. Finally, complexity, describes the similarity between the signal and a pure sine wave signal [147].

- Skewness:

  It provides information about the symmetry of the brain wave.

- Kurtosis:

  Kurtosis reflects the flattening of the signals, which means it quantifies whether the data appears flatter (or less flat) compared to the normal distribution.

2. **Power Features**

   The power spectrum feature was estimated using the modified periodogram algorithm, named the Welch method. In order to compute this feature, the data is first decomposed into successive blocks and then a periodogram is built up for each one. Lastly, the mean is calculated by assuming the average over the blocks.

3. **Entropy Features**

   The EEG signal is non-linear in nature, thus it is equally important to extract features, such as entropy, that represent this dynamic [139]. Five variants of entropy were considered in this analysis:

   - Permutation entropy (PE):

     The EEG signal is fragmented into a sequence of patterns (motifs) [148]. These motifs are assigned to one of six categories and the occurrence probability of each motif (p_i) is computed. Then PE is calculated using the standard Shannon uncertainty formula (Equation 4.2).

     $$PE = -\frac{\sum p_i \times ln(p_i)}{ln\,(number\ of\ motifs)} \tag{4.2}$$

   - Spectral entropy (SE):

     SE is defined as the Shannon entropy of the power spectral density (PSD) and describes the uniformity of the power spectral distribution [139]. It is calculated according to

Equation 4.3, where f_n is the half of the sampling frequency following the Nyquist criteria.

$$SE = -\sum_{f_n}^{f=0} PSD(f)\, log_2(PSD(f)) \tag{4.3}$$

- Singular value decomposition entropy (SVDE):

  SVDE quantifies the dimensionality of the data, indicating the number of eigenvectors required to represent the signal.

- Approximate entropy (ApEn) & Sample entropy (SampEn):

  Both measure irregularity and complexity in EEG time-series data.

  ApEn analyses how predictable is the subsequent amplitude value of the data series by knowing the previous amplitude values [149]. For example, considering a completely regular data series, the recognition of the preceding values allows a prediction of the subsequent value, which leads to an ApEn value of zero. By rising irregularity, the prediction becomes less effective, and consequently, the value of the ApEn increases.

  SampEn is an improved version of ApEn, since it is independent of data length.

4. **FD Features**

In FD the EEG signals are considered as a geometric figure, thus the geometric complexity, its correlation and evolutionary features are estimated by quantifying the fractal spaces occupied [139]. Within the several existing algorithms to compute FD, those proposed by Katz [150], Petrosian [151] and Higuchi [152] are extensively used for EEG signal characterization [153] and therefore, were the ones applied in this study.

- Katz's FD:

  This algorithm is supported by the FD calculation of a planar curve waveform. The calculation is represented by Equation 4.4 in which d is the maximum distance between two points, also associated as curve diameter, and L is the total length of the curve.

$$FD = \frac{log(L)}{log(d)} \tag{4.4}$$

- Petrosian FD:

  This method is based on the transformation of time series data into binary sequences. Once converted, FD is calculated using (Equation 4.5):

$$FD = \frac{log(n)}{log(n) + log(\frac{n}{n+0.4N_\delta})} \tag{4.5}$$

  where n is the length of the sequence and N_δ is the number of signal changes in the binary sequence.

- Higuchi's FD:

  In this method, the EEG signal is decomposed into a new self-similar time series X_k^m with N samples of progressively reduced sampling frequency. Then the signal length, $L_m(k)$, is calculated for each of the k time series X_k^m (Equation 4.6), where m denotes the initial sample.

$$L_m(k) = \frac{1}{k}\left(\sum_{i=1}^{[\frac{N-m}{k}]} abs(x(m+ik) - x(m+(i-1)k))\right)\frac{N-1}{[\frac{N-m}{k}]k} \tag{4.6}$$

  All signal lengths, $L_m(k)$, are considered and the average value of the signal length, $L(k)$, is obtained for each $k = 2, ..., k_{max}$:

$$L(k) = \frac{1}{k}\sum_{m=1}^{k} L_m(k) \tag{4.7}$$

  Finally, FD is calculated according to Equation 4.8.

$$FD = -\lim_{k\to\infty}\frac{log(L(k))}{log(k)} \tag{4.8}$$

5. **EMD Features**

   EMD separates EEG signals into a set of Intrinsic Mode Functions (IMFs) using an automatic shifting process. It is intended that each IMF represents different frequency components of the original signals so that the number of endpoints and zero-crossings must be equal or different at most by one and, at each point, the mean value estimated through the upper and lower envelope must be null [154].

   During this study, three features that describe the IMF over time, frequency and energy domain were extracted.

   - First Difference of IMF Time Series (D_t):

     It characterizes the intensity of the signal change in the time domain. Considering an IMF with N points, $IMF\{imf_1, imf_2, ..., imf_N\}$, it is calculated as:

$$D_t = \frac{1}{N-1}\sum_{n=1}^{N-1} |imf(n+1) - imf(n)| \tag{4.9}$$

   - First Difference of IMF's Phase (D_p):

     D_p depicts the intensity of phase change, or in other words, the instantaneous frequency. It is defined by Equation 4.10, where φ symbolises the instantaneous frequency.

$$D_p = \frac{1}{N-1}\sum_{n=1}^{N-1} |\varphi(n+1) - \varphi(n)| \tag{4.10}$$

- Normalized Energy of IMF (E_{norm}):

  E_{norm} accounts for the weight of the current oscillation component and is computed using Equation 4.11, where $s(n)$ is the original EEG signal point. In addition to E_{norm}, its logarithm was also considered as a feature.

$$E_{norm} = \frac{\sum_{n=1}^{N} imf^2(n)}{\sum_{n=1}^{N} s^2(n)} \tag{4.11}$$

4.2.2.4 Feature Selection and Dimensionality Reduction & Classification

Since the data analysis of both Leap Motion and Neurosky are supported on the same concepts, the dimensionality reduction, feature selection and classification followed the procedures described in Sections 4.1.2.3 and 4.1.2.4.

Given that the amount of data in these data sets was smaller, the number of folds used in the cross-validation of the grid search for hyper-parameter optimisation had to be changed to 5.

Furthermore, it is important to note that the feature selection in this data has an enhanced role due to the larger number of features extracted.

4.2.3 Application

Given the reasons explained in Section 4.1.3, for this sensor a real time test is as well required. Both approaches mentioned in that section were also considered for this sensor. Being chosen in a first instance the same test used for Leap Motion, develop an application where it could be possible to control a robot using the sensor under study.

This was the first technique followed, however due to the incompatibility felt between the Python versions of acquisition and processing, this could not reach conclusive results. Consequently, a new alternative was found to validate the proposed model, perform a new data acquisition, and determine the respective label. For this test it was intended to use the participant that could have a more statistically significant data set, and then implement its model with better performance for the classification.

Chapter 5

Results and Discussion

This chapter presents the discussion and results obtained during this dissertation. As in the previous chapters, it is divided into two main sections, one for each sensor.

Furthermore, it is important to mention that Python version 3.8 was the software used to collect and process the Leap Motion data. While for NeuroSky, the data was acquired in Python version 2.7 and processed in version 3.6, since some libraries required for processing are only available in versions higher than 3.

5.1 Leap Motion

Leap Motion data were acquired while the subjects performed a pre-defined movement for each direction, as explained in Section 4.1.1.

During this acquisition process, and even though the acquisition protocol was the same for all participants, it was possible to identify a factor that made the data differ from participant to participant - the hand tremors. Some volunteers presented noticeable hand tremors. This difference can be perceived in Figures 5.1 and 5.2.

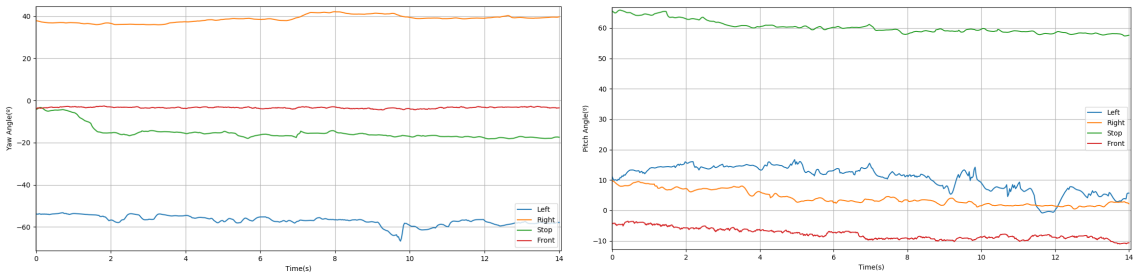

(a) Yaw Angle (b) Pitch Angle

Figure 5.1: Representation of the angles for each movement performed by a user without hand tremors.

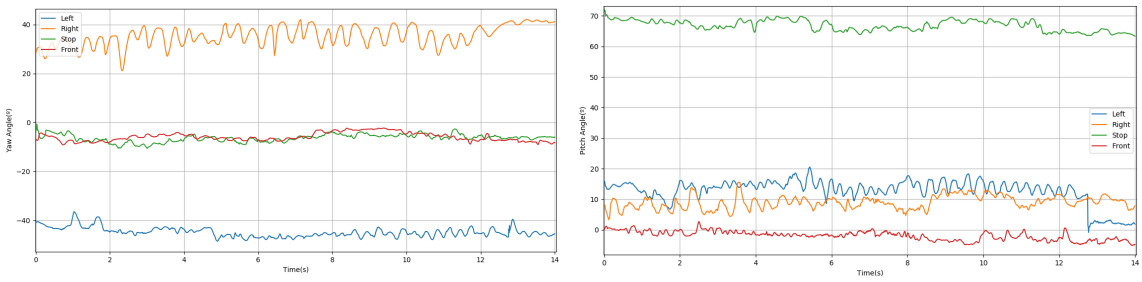

(a) Yaw Angle (b) Pitch Angle

Figure 5.2: Representation of the angles for each movement performed by a user with hand tremors.

Succinctly, when the subject has more hand tremors, this leads to data unsteadiness, as shown in the previous Figures. However, this variation happens essentially in the same range. For example, in the left-hand movement, the pitch angle could change, but it is still the direction with the lowest pitch angle value. In addition, the palm velocities were also considered as features to reduce this problem.

5.1.1 Data set

After all classifiers were trained with the data related to each participant, the best results were recorded, and they are presented in Table 5.1. Every participant has a high F1-Score value, greater than 0.97, which are excellent results given that 1 is the maximum value.

Table 5.1: F1-score for the data related to each participant.

Subject	F1 - Score	Classifier	Feature Scaling Technique
1	1	MLP	Standardization
2	0,99	MLP	Standardization
3	0,99	MLP	Standardization
4	0,98	MLP	Standardization
5	0,97	MLP	Standardization

Regarding the classifiers, MLP was the one that led to the best classification. However, as can be seen in Appendix B, Table B.1 (table with the results of all the classifiers for each participant), several classifiers exhibit similar or extremely close results. In terms of the feature scaling technique used, it is evident that the standardization of features achieves the best performances.

Analysing the confusion matrix of the best participant, in this case the number 1, it is possible to conclude that, firstly as indicated by the F1-Score value, all samples had the class correctly assigned. Second, the test set is composed of approximately the same number of samples from each class (Figure 5.3) which further reinforces the success of this classification.

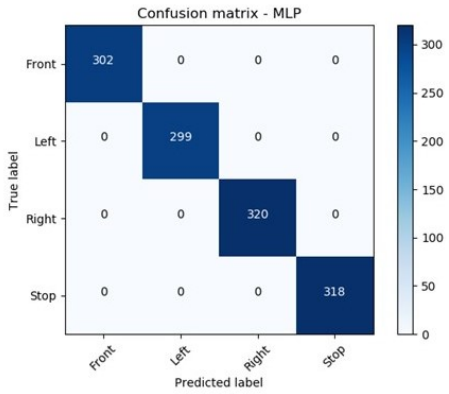

Figure 5.3: Confusion matrix of the participant with the best results.

For understanding the feasibility of developing a generic model instead of a personalised version for each patient, the data of all participants was randomly organised and the classifiers were trained. The results obtained are shown in Table 5.2.

Table 5.2: F1-score for all participants' data.

		F1 - Score	Classifier	Feature Scaling Technique
Best model		0,983	RF	Standardization
Voting	Hard	0,982	RF + MLP	Standardization
	Soft	0,984		
AdaBoost		0,982	RF	Standardization

Under this scenario, the number of samples has increased from 6 000 to 30 000. Nevertheless, the results are equally great. The best performance belongs to an Ensemble method, Voting Soft, where the RF and MLP models are the estimators considered. Through the confusion matrix of this classifier, Figure 5.4, it could be noted that the samples with wrong predicted classes are mainly Right and Stop, although in a low number. The cause of this misclassification could stem from a tendency for people to perform the Stop movement with a small deviation to Right.

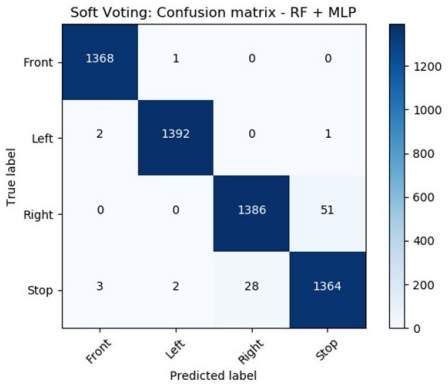

Figure 5.4: Confusion Matrix of the Voting Soft Classifier with data from all participants.

5.1.2 Real Time Application

Subject 1 obtained the best classification as concluded from Table 5.1. Hence, he was the participant selected for the real-time testing. The system consists of applying the stored MLP classifier on the extracted standardized features.

During this experiment, the participant was asked to control a robot using the same gestures that he performed in the data acquisition process.

Figure 5.5 illustrates the application developed for testing and the setup used. The track in grey corresponds to the path to follow having two stops indicated by the STOP sign. The object in blue is intended to simulate a wheelchair.

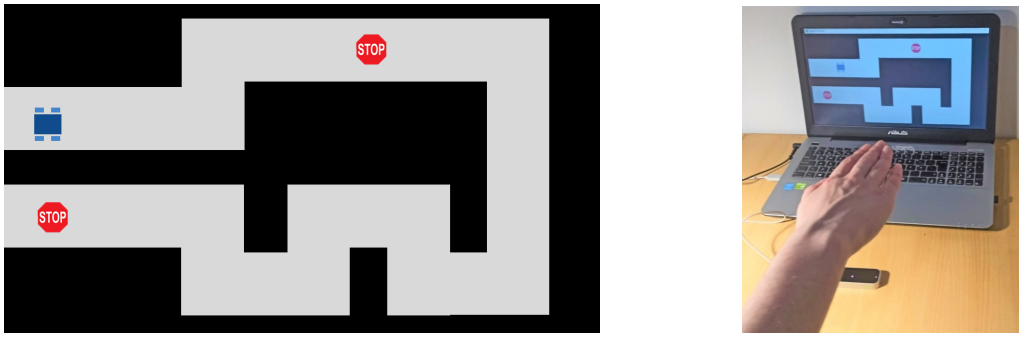

(a) Application developed

(b) Experimental Setup

Figure 5.5: Real-time testing.

In the participant's first contact with the application, he demonstrated some problems in controlling the robot, since the application has some specificities. For example, when the command assigned is left/right the robot turns 30º, so if a 90º rotation is intended, the subject needs to perform 3 times the gesture for that direction. Moreover, the assigned command takes about 1 second to be processed and executed which could induce some confusion. For this reason, a training phase was required.

After the adaptation phase, the subject was able to drive the robot during the whole route almost without leaving the grey section. Only 3 misclassifications were noticed, while the participant executed the forward class the model assigned the stop class.

To conclude, this were extremely promising results which proved the success and feasibility of using this sensor for wheelchair driving.

5.2 NeuroSky Mindwave Mobile 2

This sensor captured EEG data from different subjects while performing multiple tasks. As explained in section 4.2, different epochs can result in improved classifications, in line with this the classification results obtained for each data set as well as for each epoch are presented below. The

detailed representation of the results for each participant and classifier can be found in Appendix B, section B.2.

It should be clarified that in Tables 5.3 -5.9, when the term "all" is mentioned, it corresponds to training the classifiers with data from all subjects. Furthermore, the terms "Stand" and "Norm" are the simplified versions of Standardization and Normalization, respectively. When a "-" appears in the feature scaling cell, it indicates that the best result was achieved without these types of techniques.

5.2.1 Data set A

This data set is related to the imaginary period with only one visual stimulus in the seconds preceding the imagination.

Table 5.3 presents the results achieved.

Table 5.3: Results of the F1-score for data set A.

	Data set A								
	Epoch 4s			Epoch 3s			Epoch 2s		
Subject	**F1-Score**	**Classifier**	**Feature Scaling**	**F1-Score**	**Classifier**	**Feature Scaling**	**F1-Score**	**Classifier**	**Feature Scaling**
1	1	MLP	Stand	0,77	MLP	-	0,79	RF	-
2	1	MLP	Stand	0,85	MLP	Stand	1	SVM	-
3	0,78	GNB	Stand	0,63	KNN	Stand	0,4	KNN	Stand
4	1	MLP	Stand	0,75	LR	Stand	0,62	DTC	-
5	0,78	MLP	Stand	0,5	MLP	Stand	0,67	MLP	Stand
6	1	MLP	Stand	0,85	SVM	Stand	0,47	KNN	Stand
7	1	MLP	Stand	0,54	MLP	Stand	0,64	LDA	Stand
8	0,67	RF	-	0,75	MLP	Stand	0,84	LR	Stand
9	1	MLP	Stand	0,77	LDA	-	0,71	LDA	Stand
10	0,78	LDA	Stand	1	RF	Stand	0,71	LSVM	Stand
11	1	LDA	Stand	0,64	MLP	Stand	0,68	LDA	Stand
12	1	MLP	Stand	1	GNB	-	0,68	LR	Stand
Mean	0,92			0,75			0,68		
All	0,35	SVM	Stand	0,3	DTC	Norm	0,3	RF	Stand

Table 5.4: Size of the training and test set of the data set A.

	Data set A					
	Epoch 4s		Epoch 3s		Epoch 2s	
	Subject	All	Subject	All	Subject	All
Train Set	11	125	15	167	23	261
Test Set	3	32	4	42	6	66

Firstly, and for a proper discussion of the results, it is also important to analyze the different sizes of the training and test sets (Table 5.4). Since the same data was split into 4s, 3s and 2s it is expected that the 2s data set has more samples than the remaining ones.

About the results, it is evident, firstly, that the maximum value of F1-Score was reached in each epoch. In the case of the 4s epoch this was obtained by several participants, in the 3s epoch only 2 reached this value and in the 2s epoch only participant 2 had the F1-Score value of 1.

Moreover, participant 2 demonstrates that even if the number of samples is increased, the results can be equally good. This can be seen by the results obtained for epochs of 4 and 2s. In that of 2s the size of the test set was double, and the result was identical.

In the feature scaling technique, it is unanimous that Standardization produces the best outcomes.

Comparing the results of using data from all participants rather than just participant-related data, a decrease in the value of the evaluation metric is noticeable. However, this is not a surprising result given that brainwaves differ from person to person.

5.2.2 Data set B

Data set B corresponds to the imagination of the different directions while a wheelchair simulator video was displayed.

The results obtained and the size of the data sets are exposed in Table 5.5 and 5.6, respectively. To highlight, during the data acquisition of participant 5, the sensor did not establish a proper connection. Consequently, the data did not have a sufficient quality for the analysis and were therefore discarded.

Table 5.5: Results of the F1-score for data set B.

	Data set B								
	Epoch 4s			Epoch 3s			Epoch 2s		
Subject	**F1-Score**	**Classifier**	**Feature Scaling**	**F1-Score**	**Classifier**	**Feature Scaling**	**F1-Score**	**Classifier**	**Feature Scaling**
1	0,81	LSVM	-	0,48	GNB	Stand	0,41	MLP	-
2	0,61	LR	Stand	0,72	LDA	-	0,5	RF	Stand
3	0,73	MLP	Stand	0,61	GNB	Stand	0,39	MLP	Stand
4	0,81	GNB	-	0,59	DTC	Stand	0,68	RF	Stand
5									
6	0,88	DTC	-	0,58	RF	Stand	0,67	LSVM	Stand
7	0,61	LDA	Stand	0,56	SVM	Norm	0,68	MLP	Stand
8	0,6	MLP	-	0,24	GNB	Stand	0,47	MLP	-
9	0,43	LDA	-	0,31	LDA	-	0,49	LR	-
10	0,88	RF	Norm	0,35	GNB	Stand	0,8	LR	-
11	0,71	LR	-	0,75	LSVM	Stand	0,47	LSVM	Stand
12	0,88	MLP	Stand	0,33	DTC	-	0,34	RF	Stand
Mean	0,72			0,50			0,54		
All	0,3	SVM	Stand	0,47	SVM	Stand	0,41	RF	Stand

Table 5.6: Size of the training and test set of the data set B.

	Data set B					
	Epoch 4s		Epoch 3s		Epoch 2s	
	Subject	All	Subject	All	Subject	All
Train Set	20	200	28	288	45	460
Test Set	5	50	8	72	12	116

From the analysis of the table, it can be concluded that the 4s epoch leads to better results. This is observed either by the F1-Score value of the participants or the average value of all participants. Concerning the classifier or feature scaling method, since the best results are scattered, it is not possible to mention which one is the best.

5.2.3 Data set C

Data set C is quite similar with the previous data set, differing only in the video shown. In this case, a video of a roller coaster is used.

The 5.7 and 5.8 tables depict the classification performance and the sizes of the data sets.

Table 5.7: Results of the F1-score for data set C.

	Data set C								
	Epoch 4s			Epoch 3s			Epoch 2s		
Subject	**F1-Score**	**Classifier**	**Feature Scaling**	**F1-Score**	**Classifier**	**Feature Scaling**	**F1-Score**	**Classifier**	**Feature Scaling**
1	0,35	LR	Norm	0,75	SVM	Norm	0,45	MLP	Stand
2	0,87	RF	-	0,81	LR	Stand	0,67	LR	Norm
3	0,79	DTC	Stand	0,75	DTC	Stand	0,5	GNB	-
4	0,8	LR	Stand	0,33	DTC	-	0,51	RF	-
5	0,8	RF	Norm	0,71	GNB	Stand	0,41	RF	-
6	0,47	MLP	Stand	0,75	MLP	-	0,53	RF	Stand
7	0,37	SVM	Norm	0,6	DTC	Stand	0,58	LR	Stand
8	0,8	DTC	Stand	0,59	LR	Stand	0,56	SVM	Stand
9	1	MLP	-	0,74	MLP	-	0,75	GNB	-
10	0,53	LDA	Stand	0,58	LSVM	Stand	0,5	LR	-
11	0,8	MLP	Stand	0,57	KNN	Norm	0,55	RF	Stand
12	0,53	DTC	Stand	0,48	DTC	Stand	0,38	LR	Stand
Mean	0,68			0,64			0,53		
All	0,31	RF	Stand	0,33	KNN	Norm	0,4	RF	Norm

For an epoch length of 4s, participant 9 exhibits the maximum F1-Score value. This had happened previously on data set A for the same epoch length. Additionally, this experiment demonstrates a preference for using standardisation for the feature scaling method and the overall results are significantly better when compared to data set B.

Table 5.8: Size of the training and test set of the data set C.

	Data set C					
	Epoch 4s		Epoch 3s		Epoch 2s	
	Subject	All	Subject	All	Subject	All
Train Set	17	199	26	298	44	487
Test Set	5	50	7	75	11	122

In contrast to data set B, in this data set the shorter the epoch time the better the classification is using all patients' data. The F1-Score value increased from 0.31 in the 4s epoch to 0.4 in the 2s epoch.

5.2.4 Data set D

The last set of data relates to driving a wheelchair along a pre-defined path. This data set presents a higher number of samples from the front class, which did not occur in the previous data sets where the classes were equally present. Although the path was defined taking into account the time spent in each class, the front class was the one that users took more time to go through, which originated this difference.

Tables 5.9 and 5.10 contain both the classification scores and the size of the test and training sets. To note that participants 9 and 10 were unable to perform this acquisition due to technical problems with the wheelchair used during the experiment.

Table 5.9: Results of the F1-score for data set D.

	Data set D								
	Epoch 4s			Epoch 3s			Epoch 2s		
Subject	**F1-Score**	**Classifier**	**Feature Scaling**	**F1-Score**	**Classifier**	**Feature Scaling**	**F1-Score**	**Classifier**	**Feature Scaling**
1	0,86	LDA	Stand	0,87	MLP	-	0,79	KNN	-
2	0,65	LDA	Stand	0,49	KNN	Norm	0,76	MLP	Norm
3	0,71	GNB	Stand	0,49	LDA	Stand	0,59	MLP	Stand
4	0,43	LSVM	Norm	0,62	DTC	Norm	0,66	KNN	Stand
5	0,9	LSVM	Stand	0,61	DTC	Stand	0,5	KNN	Norm
6	0,79	MLP	Stand	0,67	RF	-	0,67	MLP	Stand
7	0,6	LSVM	Norm	0,72	LR	Stand	0,52	RF	Norm
8	1	LDA	Stand	0,89	LDA	Stand	0,75	GNB	Stand
9									
10									
11	0,77	LDA	Stand	0,81	RF	-	0,68	MLP	-
12	0,68	GNB	Stand	0,52	MLP	-	0,6	LDA	Stand
Mean	0,74			0,67			0,65		
All	0,51	LDA	-	0,44	RF	-	0,41	RF	Stand

Table 5.10: Size of the training and test set of the data set D.

	Data set D					
	Epoch 4s		Epoch 3s		Epoch 2s	
	Subject	All	Subject	All	Subject	All
Train Set	28	349	41	512	70	855
Test Set	7	88	11	128	18	214

This data set is the one with the highest F1-Score value for each epoch. Comparing all participants, the 8 had a better performance for the 3 temporal segments considered. Moreover, a slight tendency is observed for the LDA model to be the one that provides a better classification.

5.2.5 General discussion

Given all the results previously described and summarised in Table 5.11, data set A appears as being the best approach to develop a model that enables users to drive an intelligent wheelchair. In this data set for all three epoch lengths, the F1-Score reaches the maximum value.

Table 5.11: Comparison of the best participant from each data set.

	Epoch 4s				Epoch 3s				Epoch 2s			
	Subject	F1 - Score	Classifier	Feature Scaling	Subject	F1 - Score	Classifier	Feature Scaling	Subject	F1 - Score	Classifier	Feature Scaling
Data set A	1,2,4,6,7,9,11,12	1	MLP, LDA	Stand	10, 12	1	RF, GNB	Stand, -	2	1	SVM	-
Data set B	6, 10, 12	0,88	DTC, RF, MLP	-, Norm, Stand	11	0,75	LSVM	Stand	10	0,8	LR	-
Data set C	9	1	MLP	-	2	0,81	LR	Stand	9	0,75	GNB	-
Data set D	8	1	LDA	Stand	8	0,89	LDA	Stand	1	0,79	KNN	-

Concerning the classifiers or the feature scaling, these changed based on the subject. However, surprisingly for a 2s epoch for all the data sets, the highest performance was provided without feature scaling. Feature scaling is usually required to suppress the effect of different magnitudes or amplitude on features.

Although the classification overall seems to be great, the data set sizes are relatively small, which could represent a statistically non-significant sample for inferring conclusions. Consequently, one of the participants, in this case the 12 for having greater availability and being within those with better results in one of the data sets, repeated the acquisition protocol for data set A six more times. This resulted in training and test sets with new sizes, as described in Table 5.12.

Table 5.12: Size of the training and test set for the new acquisition of subject 12 to the data set A.

	Epoch 4s	Epoch 3s	Epoch 2s
Train Set	75	108	162
Test Set	19	27	41

After training these new data, new performances were generated, as can be seen by the F1-Score values shown in Table 5.13.

Table 5.13: Results of the F1-score for the new acquisition of subject 12 to the data set A.

		Data set A (Subject 12)								
		Epoch 4s			Epoch 3s			Epoch 2s		
		F1 - Score	Classifier	Feature Scaling	F1 - Score	Classifier	Feature Scaling	F1 - Score	Classifier	Feature Scaling
1 model		0,48	KNN	Stand	0,39	RF	Stand	0,38	RF	-
Voting	Hard	0,48	KNN + SVM	Stand	0,37	RF + GNB	Stand	0,33	LDA + RF	Stand
	Soft	0,4			0,39			0,43		
AdaBoost		0,27	SVM	Stand	0,37	RF	Stand	0,35	RF	-

The classification was less efficient which was reflected in lower values of the evaluation parameter. To illustrate how the assignment of classes was carried out, the confusion matrix for the best result was represented in Figure 5.6, in this case the 4s epoch with the K-NN classifier, which consists of an F1-Score value of 0.48.

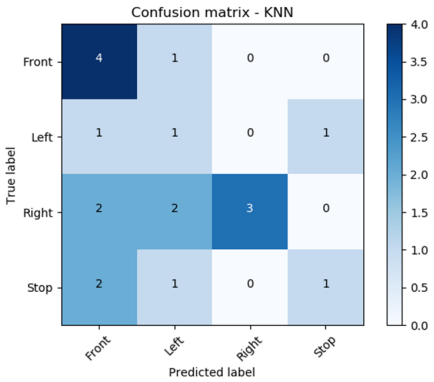

Figure 5.6: Confusion matrix of the K-NN classifier for a 4s epoch of participant 12.

It can be concluded that the front and right classes were the most easily identified while the left and stop directions were more challenging.

During this study F1-Score was used as the evaluation metric, due to the fact that FN and FP play a key role. However, to compare with other authors' work, accuracy was also estimated. Thereby for the F1-Score result of 0.48 with the K-NN classifier (subject 12 epoch of 4s) a total accuracy of 47% was achieved, or more specifically 80%, 33%, 43% and 25% for the classes Front, Left, Right and Stop.

Permana et al., 2019 [155] proposed a wheelchair controlled by also using this sensor where the four classes consisted of: move forward (think forward), backward (think backward), turn left (think backward while constantly moving their eyes) and turn right (think forward while continuously moving their eyes). This approach enabled them to have a total accuracy rate of 52-56% (depending on the participant) and 82%, 70%, 73%, 47% and 18% when the success rate for each class was considered.

These results, not as satisfactory as desired, may stem from several factors. Firstly, the acquisition was conducted on different days, i.e. the first acquisition protocol was done on one day

and then the repetitions were consecutively performed on another day, which could have caused brain exhaustion. Secondly, a higher level of fatigue could have occurred on the repetition day leading to a greater difficulty in concentration and consequently a poorer data quality. Thirdly, the extracted features may still not be the most suitable for this patient.

In the literature it is also possible to find some studies with higher levels of accuracy for the classification, however most of them used attention and concentration levels as features, which was not the goal of this study.

5.2.6 Application

Having into account the different data sets, classifiers and participants, subject 12 was the one selected to perform this test in real-time.

Firstly, it was with him that the new data acquisition was carried out in order to have a statistically significant data set. Secondly, he was among the most available for continuing to contribute to this study, although the performance of his best model is medium (Table 5.13).

Once the model is verified to work minimally on a patient where performance is not the highest this will validate the proof of concept.

Therefore, 24 samples of 4 seconds were recorded following the acquisition protocol for data set A (Section 4.2.1.1). After that, the samples were classified using the K-NN model and feature standardization, the combination that appears to be the best for this participant (Table 5.13).

The class allocated to each sample, and its true label, are presented in Table 5.14.

Through the Table, it can quickly be seen that the classification was not satisfactory, only 6 of the 24 samples were classified correctly. Having verified a greater ability to hit the classifications Front and Right, which was already expected since in the confusion matrix (Figure 5.6) were also the most identified classes.

Nevertheless, during the acquisition, the subject presented some problems in thinking about direction because it was a period of time so short that he could not concentrate appropriately. For this reason, just to evaluate the performance in longer temporal segments where the subject could be more focused, data acquisition for 10s was also collected. Table 5.15 displays the results obtained for this epoch length.

Although the model was trained for 4s it appears to be more effective in larger temporal segments, it was able to classify 6 from the 16 samples. This could be explained by the fact that in a longer temporal segment the participant is able to be more conscious to imagine the direction. During the acquisition of the data for training, this limitation was not felt since 15s was acquired and then these were divided into the intended temporal segments.

In summary, this could be a promising approach, but it still requires some improvements. Firstly, misclassifications cannot occur in real time, this could endanger the life of the IW user. Moreover, 10s segments are too long for a real-time implementation.

Table 5.14: Classification of the data set for validation of participant 12 with an epoch length of 4s.

Epoch 4s		
Test Set File	**Label**	**Predict**
1	Front	Front
2	Right	Left
3	Left	Stop
4	Stop	Left
5	Front	Left
6	Right	Right
7	Left	Right
8	Stop	Right
9	Front	Front
10	Right	Stop
11	Left	Stop
12	Stop	Front
13	Front	Left
14	Right	Right
15	Left	Right
16	Stop	Right
17	Front	Front
18	Right	Left
19	Left	Front
20	Stop	Front
21	Front	Left
22	Right	Left
23	Left	Front
24	Stop	Stop

Front:	3 / 6
Right:	2 / 6
Left:	0 / 6
Stop:	1 / 6

Total:	6 / 24

Table 5.15: Classification of the data set for validation of participant 12 with an epoch length of 10s.

Epoch 10s		
Test Set File	**Label**	**Predict**
1	Front	Front
2	Right	Right
3	Left	Right
4	Stop	Left
5	Front	Right
6	Right	Right
7	Left	Front
8	Stop	Front
9	Front	Front
10	Right	Left
11	Left	Front
12	Stop	Left
13	Front	Front
14	Right	Right
15	Left	Front
16	Stop	Left

Front:	3 / 4
Right:	3 / 4
Left:	0 / 4
Stop:	0 / 4

Total:	6 / 16

Chapter 6

Conclusion

6.1 General conclusions

Different health conditions imply the existence of multiple alternatives for the interaction between a human and a machine, replacing the traditional modes of communication. Consequently, manual wheelchairs are no longer viable solutions for everyone; therefore, with the trend towards an increasingly technological world, different options have emerged, especially that of IW.

Several commercial sensors can be found on the market, however some features such as level of invasiveness, shape, price, ease of use and accuracy should be carefully analyzed for a proper choice. Hence, Leap Motion and NeuroSky Mindwave Mobile 2 were selected.

During this dissertation, these two sensors were carefully analyzed to decode the user's intention on one of four fundamental control commands for an IW, move forward, turn left, right or stop. This user desire was assigned, in the case of Leap Motion by interpreting hand gestures while in NeuroSky it is based on recognition of this thought in brain waves.

Through the proposed methodologies, Leap Motion achieves an optimal result, an F1-Score greater than 0.97. Moreover, it performed really well in the real-time application, being possible to control a robot on a path.

NeuroSky did not demonstrate so much success. Comparing the four data sets created, the one that showed the best results was A. This suggests that imagining a certain direction after observing an arrow indicating that direction provides a better classification than having no stimulus or having a stimulus in video format. Hence an average F1-Score of 0.92, 0.75 and 0.68 was obtained for the epochs of length 4s, 3s and 2s, respectively.

Therefore, and to increase the number of samples, the best participant of this data set (user 12) repeated the respective acquisition protocol. Thus, a model was created for classification with an F1-Score of 0.48. When tested in real time, this algorithm proved not to work as intended since it could only correctly identify 6 of the 24 test samples.

In general, it is noticed that feature standardization leads to higher performances when compared to other scaling techniques. In addition, better classifications can also be achieved when

training the models only with data from one patient than with data from all patients. An expected conclusion because brain waves are specific to each person.

Despite the satisfactory results obtained, some difficulties were experienced in this work, namely the communication between the different python versions used and the data acquisition. In terms of python versions, this limitation was more noticeable in NeuroSky since data acquisition required Python 2.7 and its processing required version 3.6. Data acquisition also became a limiting point due to the pandemic situation at that time, as it became more complicated to find volunteers for the study.

To conclude, although the results were more successful with Leap Motion than with NeuroSky, the possibility of controlling an IW using hand gesture recognition and brainwave analysis was supported. These are promising approaches that, with improvements, could be incorporated into a real IW.

6.2 Future work

During this dissertation, a proof of concept was developed for both sensors. However, the system can still be optimized, and its functioning improved, especially the NeuroSky Sensor part. For this reason, the first step of future work should fall on the conversion of both developed algorithms to the same Python version, where they could be tested, as well as integrated into the IW multimodal interface.

In respect to Leap Motion, real time tests have revealed to be quite successful. Hence, the next phase consists in studying the position as well as building the support to implement it in an IW. This position will depend on whether the patient is right or left-handed. Nevertheless, this sensor could provide more inclusive solutions, this means that it could be further investigated, and a customized gesture system could be developed to be adaptable to the different needs and health conditions of each patient. Furthermore, new gestures could be implemented to enable IW communication with, for example, home devices. This would result in a more versatile and functional system.

Concerning the NeuroSky sensor, it is recommended to perform a more generalized acquisition, as well as an acquisition on people with some health problems. This would provide more reliable conclusions about the performance of this single channel headset on anyone regardless of health condition. After that, a further analysis needs to be done in real time to estimate what is the possible delay in classification caused by both epoch length and data processing.

Finally, once all models are operating properly, they could be integrated and tested on a multimodal interface of a real IW.

References

[1] A Davies, LH De Souza, and AO Frank. "Changes in the quality of life in severely disabled people following provision of powered indoor/outdoor chairs". In: *Disability and Rehabilitation* 25.6 (2003), pp. 286–290.

[2] Alicia M Koontz et al. *Wheeled mobility*. 2015.

[3] *Guidelines on the provision of manual wheelchairs in less resourced settings*. URL: https://www.who.int/publications/i/item/guidelines_on_the_provision_of_manual_wheelchairs_in_less_resourced_settings (visited on 02/01/2021).

[4] *Worldwide Need - Wheelchair Foundation*. URL: https://www.wheelchairfoundation.org/fth/analysis-of-wheelchair-need/ (visited on 02/01/2021).

[5] Gordon Tao et al. "Evaluation tools for assistive technologies: a scoping review". In: *Archives of Physical Medicine and Rehabilitation* 101.6 (2020), pp. 1025–1040.

[6] *ISO 9999:2016(en), Assistive products for persons with disability — Classification and terminology*. URL: https://www.iso.org/obp/ui#iso:std:iso:9999:ed-6:v1:en:term:2.13 (visited on 12/21/2020).

[7] Luís Azevedo. *As Tecnologias de Informação e Comunicação e as Necessidades Especiais*. Diversidades, 2005.

[8] M Donnelly. "Assistive Technology in Education". In: *EBSCO Research Starters* (2008), pp. 1–6.

[9] A Edward Blackhurst. "Perspectives on applications of technology in the field of learning disabilities". In: *Learning Disability Quarterly* 28.2 (2005), pp. 175–178.

[10] Maria Clarisse Alexandrino Nunes. "Apoio a pais e docentes de alunos com multideficiência: Conceção e desenvolvimento de um ambiente virtual de aprendizagem". PhD thesis. Universidade de Lisboa, 2012. URL: https://repositorio.ul.pt/bitstream/10451/7702/1/ulsd064599_td_tese.pdf.

[11] Åse Brandt, Susanne Iwarsson, and Agneta Ståhle. "Older people's use of powered wheelchairs for activity and participation". In: *Journal of rehabilitation medicine* 36.2 (2004), pp. 70–77.

[12] Jesse Leaman and Hung Manh La. "A comprehensive review of smart wheelchairs: past, present, and future". In: *IEEE Transactions on Human-Machine Systems* 47.4 (2017), pp. 486–499.

[13] *What is the definition of a wheelchair under the ADA? | ADA National Network*. URL: https://adata.org/faq/what-definition-wheelchair-under-ada (visited on 12/22/2020).

[14] Brígida Mónica Faria, Luís Paulo Reis, and Nuno Lau. "A survey on intelligent wheelchair prototypes and simulators". In: *New Perspectives in Information Systems and Technologies, Volume 1*. Springer, 2014, pp. 545–557.

[15] Cathy Brighton. "Rules of the road." In: *Rehab management* 16.3 (2003), pp. 18–21. ISSN: 08996237.

[16] Pooja Viswanathan et al. "Intelligent wheelchair control strategies for older adults with cognitive impairment: user attitudes, needs, and preferences". In: *Autonomous Robots* 41.3 (2017), pp. 539–554.

[17] Dirk Vanhooydonck et al. "Adaptable navigational assistance for intelligent wheelchairs by means of an implicit personalized user model". In: *Robotics and Autonomous Systems* 58.8 (2010), pp. 963–977.

[18] Brigida Monica Faria, Luis Paulo Reis, and Nuno Lau. "Cerebral palsy eeg signals classification: Facial expressions and thoughts for driving an intelligent wheelchair". In: *2012 IEEE 12th International Conference on Data Mining Workshops*. IEEE. 2012, pp. 33–40.

[19] Sarah Frost et al. *Wheelchair Service Training Package Reference Manual for Participants Intermediate Level*. Section A. Core Knowledge. World Health Organization, 2013. ISBN: 9789241505765.

[20] *Proposta de Candidatura - Sistema de Incentivos à Investigação e Desenvolvimento Tecnológico (SI I&DT)*. Tech. rep. IntellWheels2.0 / Anexo Técnico – Aviso 31/SI/2017.

[21] Paulo Gurgel Pinheiro, Cláudio Gurgel Pinheiro, and Eleri Cardozo. "The Wheelie—A facial expression controlled wheelchair using 3D technology". In: *2017 26th IEEE International Symposium on Robot and Human Interactive Communication (RO-MAN)*. IEEE. 2017, pp. 271–276.

[22] Louise Devigne et al. "Power wheelchair navigation assistance using wearable vibrotactile haptics". In: *IEEE transactions on haptics* 13.1 (2020), pp. 52–58.

[23] *The Maker: George Klein and the first electric wheelchair - U of T Engineering News*. URL: https://news.engineering.utoronto.ca/maker-george-klein-first-electric-wheelchair/ (visited on 01/11/2021).

[24] Richard L. Madarasz et al. “The Design of an Autonomous Vehicle for the Disabled”. In: *IEEE Journal on Robotics and Automation* 2.3 (1986), pp. 117–126. ISSN: 08824967. DOI: 10.1109/JRA.1986.1087052. URL: http://ieeexplore.ieee.org/document/1087052/.

[25] Helmut Hoyer and Ralf Hoelper. “Open Control Architecture for an Intelligent Omni-Directional Wheelchair”. In: *Proc. 1st TIDE Congress, Brussels* (1993), pp. 93–97.

[26] Filipe Joaquim de Oliveira Reis Coelho. “Multimodal Interface for an Intelligent Wheelchair”. PhD thesis. Faculdade de Engenharia da Universidade do Porto, 2019.

[27] Ulrich Borgolte et al. “Architectural Concepts of a Semi-autonomous Wheelchair”. In: *Journal of Intelligent and Robotic Systems: Theory and Applications* 22.3-4 (1998), pp. 233–253. ISSN: 09210296. DOI: 10.1023/a:1007944531532. URL: https://link.springer.com/article/10.1023/A:1007944531532.

[28] Parris Wellman, Venkat Krovi, and Vijay Kumar. “An adaptive mobility system for the disabled”. In: *Proceedings - IEEE International Conference on Robotics and Automation*. pt 3. Publ by IEEE, 1994, pp. 2006–2011. ISBN: 0818653329. DOI: 10.1109/robot.1994.351169.

[29] Simon P Levine et al. *The NavChair Assistive Wheelchair Navigation System*. Tech. rep. 4. 1999, p. 443.

[30] David P. Miller and Marc G. Slack. “Design and testing of a low-cost robotic wheelchair prototype”. In: *Autonomous Robots* 2.1 (1995), pp. 77–88. ISSN: 09295593. DOI: 10.1007/BF00735440. URL: https://link.springer.com/article/10.1007/BF00735440.

[31] Daniel José Fernandes Dias. “Interação multimodal de dispositivos robóticos em ambiente simulado”. PhD thesis. Universidade do Minho, 2015.

[32] Bernhard Borgerding et al. “FRIEND: Functional robot arm with user friendly interface for disabled people”. In: *The 5th European Conference for the Advancement of Assistive Technology, accepted for publishing*. 1999.

[33] Ivan Volosyak, Oleg Ivlev, and Axel Graser. “Rehabilitation robot FRIEND II-the general concept and current implementation”. In: *9th International Conference on Rehabilitation Robotics, 2005. ICORR 2005.* IEEE. 2005, pp. 540–544.

[34] Brice Rebsamen et al. “A brain-controlled wheelchair based on P300 and path guidance”. In: *The First IEEE/RAS-EMBS International Conference on Biomedical Robotics and Biomechatronics, 2006. BioRob 2006.* IEEE. 2006, pp. 1101–1106.

[35] Cuntai Guan, Manoj Thulasidas, and Jiankang Wu. “High performance P300 speller for brain-computer interface”. In: *IEEE International Workshop on Biomedical Circuits and Systems, 2004.* IEEE. 2004, S3–5.

[36] Borja Bonail, Julio Abascal, and Luis Gardeazabal. “Wheelchair-based open robotic platform and its performance within the ambiennet project”. In: *Proceedings of the 2nd International Conference on PErvasive Technologies Related to Assistive Environments*. 2009, pp. 1–6.

[37] Luís Paulo Reis et al. “Multimodal interface for an intelligent wheelchair”. In: *Informatics in Control, Automation and Robotics*. Springer, 2015, pp. 1–34.

[38] Rodrigo AM Braga et al. “Intellwheels-a development platform for intelligent wheelchairs for disabled people”. In: *ICINCO 2008: PROCEEDINGS OF THE FIFTH INTERNATIONAL CONFERENCE ON INFORMATICS IN CONTROL, AUTOMATION AND ROBOTICS, VOL RA-2: ROBOTICS AND AUTOMATION, VOL 2*. 2008.

[39] Pedro Miguel Faria et al. “Interface framework to drive an intelligent wheelchair using facial expressions”. In: *2007 IEEE International Symposium on Industrial Electronics*. IEEE. 2007, pp. 1791–1796.

[40] *Wheelie – Control Motorized Wheelchair with Facial Expressions*. URL: https://www.intel.com/content/www/us/en/artificial-intelligence/videos/hoobox-wheelie-video.html (visited on 02/02/2021).

[41] Robert Lievesley, Martin Wozencroft, and David Ewins. “The Emotiv EPOC neuroheadset: an inexpensive method of controlling assistive technologies using facial expressions and thoughts?” In: *Journal of Assistive Technologies* (2011).

[42] Minglu Zhu, Tianyiyi He, and Chengkuo Lee. “Technologies toward next generation human machine interfaces: From machine learning enhanced tactile sensing to neuromorphic sensory systems”. In: *Applied Physics Reviews* 7.3 (2020), p. 031305.

[43] Vladimir I Pavlovic, Rajeev Sharma, and Thomas S. Huang. “Visual interpretation of hand gestures for human-computer interaction: A review”. In: *IEEE Transactions on pattern analysis and machine intelligence* 19.7 (1997), pp. 677–695.

[44] Hobeom Han and Sang Won Yoon. “Gyroscope-Based Continuous Human Hand Gesture Recognition for Multi-Modal Wearable Input Device for Human Machine Interaction”. In: *Sensors* 19.11 (2019), p. 2562.

[45] Sushmita Mitra and Tinku Acharya. “Gesture recognition: A survey”. In: *IEEE Transactions on Systems, Man, and Cybernetics, Part C (Applications and Reviews)* 37.3 (2007), pp. 311–324.

[46] Salah Bourennane and Caroline Fossati. “Comparison of shape descriptors for hand posture recognition in video”. In: *Signal, Image and Video Processing* 6.1 (2012), pp. 147–157.

[47] GRS Murthy and RS Jadon. “A review of vision based hand gestures recognition”. In: *International Journal of Information Technology and Knowledge Management* 2.2 (2009), pp. 405–410.

[48] Paulo Trigueiros, Fernando Ribeiro, and Luís Paulo Reis. "Hand Gesture Recognition System based in Computer Vision and Machine Learning". In: *Developments in Medical Image Processing and Computational Vision*. Springer, 2015, pp. 355–377.

[49] Zhong Shen et al. "A soft stretchable bending sensor and data glove applications". In: *Robotics and biomimetics* 3.1 (2016), p. 22.

[50] *Simple Hand Gesture Recognition Code - Hand tracking - Mediapipe · GitHub*. URL: https://gist.github.com/TheJLifeX/74958cc59db477a91837244ff598ef4a (visited on 01/15/2021).

[51] Md Hasanuzzaman et al. "Real-time vision-based gesture recognition for human robot interaction". In: *2004 IEEE International Conference on Robotics and Biomimetics*. IEEE. 2004, pp. 413–418.

[52] *How It Works: Xbox Kinect*. URL: https://www.jameco.com/Jameco/workshop/Howitworks/xboxkinect.html (visited on 01/16/2021).

[53] *Intel® RealSense™ Technology*. URL: https://www.intel.com/content/www/us/en/architecture-and-technology/realsense-overview.html (visited on 01/16/2021).

[54] *GestIC Gesture Recognition Controller Uses Electrical Fields: Science Fiction in the News*. URL: http://www.technovelgy.com/ct/Science-Fiction-News.asp?NewsNum=3823 (visited on 01/16/2021).

[55] *Tracking | Leap Motion Controller | Ultraleap*. URL: https://www.ultraleap.com/product/leap-motion-controller/ (visited on 01/16/2021).

[56] Jade Sciberras. "Interactive Gesture Controller for a Motorised Wheelchair". PhD thesis. Murdoch University, 2015.

[57] *Kinect - Windows app development*. URL: https://developer.microsoft.com/en-us/windows/kinect/ (visited on 01/16/2021).

[58] Microchip. *MGC3030/3130 3D Tracking and Gesture Controller Data Sheet*. Tech. rep. URL: http://ww1.microchip.com/downloads/en/DeviceDoc/MGC3030-3130-3D-Tracking-and-Gesture-Controller-40001667F.pdf.

[59] *GestIC Technology Basics | Microchip Technology*. URL: https://www.microchip.com/design-centers/capacitive-touch-sensing/gestic-technology/gestic-technology-basics (visited on 01/16/2021).

[60] Michael Van den Bergh et al. "Real-time 3D hand gesture interaction with a robot for understanding directions from humans". In: *2011 Ro-Man*. IEEE. 2011, pp. 357–362.

[61] Luca Montanaro et al. "A Touchless Human-machine Interface for the Control of an Elevator." In: *RTA-CSIT*. 2016, pp. 58–65.

[62] D Chaitanya and Y Aruna Suhasini. *Home Appliances Control Based on Hand Motion Gesture*. 2017. URL: www.ijeter.everscience.org.

[63] Dae-Sung Park et al. “Effects of virtual reality training using Xbox Kinect on motor function in stroke survivors: a preliminary study”. In: *Journal of Stroke and Cerebrovascular Diseases* 26.10 (2017), pp. 2313–2319.

[64] Bo Liao et al. “Hand gesture recognition with generalized hough transform and DC-CNN using realsense”. In: *2018 Eighth International Conference on Information Science and Technology (ICIST)*. IEEE. 2018, pp. 84–90.

[65] Zhenfei Zhao et al. “Web-based interactive drone control using hand gesture”. In: *Review of Scientific Instruments* 89.1 (2018), p. 014707.

[66] Yuanyuan Feng et al. “Comparison of Kinect and Leap Motion for Intraoperative Image Interaction”. In: *Surgical Innovation* (2020), p. 1553350620947206.

[67] Shahin Fereidouni et al. “A novel design and implementation of wheelchair navigation system using Leap Motion sensor”. In: *Disability and Rehabilitation: Assistive Technology* (2020), pp. 1–7.

[68] Ultraleap. *Leap Motion Controller TM*. Tech. rep. URL: https://www.ultraleap.com/datasheets/Leap_Motion_Controller_Datasheet.pdf.

[69] *How Hand Tracking Works | Ultraleap*. URL: https://www.ultraleap.com/company/news/blog/how-hand-tracking-works/ (visited on 01/17/2021).

[70] Sérgio Afonso. “Development of a Gestural Master Interface for Tele-Surgery Applications”. PhD thesis. Instituto Superior Técnico, 2014.

[71] *System Architecture — Leap Motion Python SDK v2.3 documentation*. URL: https://developer-archive.leapmotion.com/documentation/v2/python/devguide/Leap_Architecture.html (visited on 01/17/2021).

[72] Thomas J Sullivan, Stephen R Deiss, and Gert Cauwenberghs. “A low-noise, non-contact EEG/ECG sensor”. In: *2007 IEEE Biomedical Circuits and Systems Conference*. IEEE. 2007, pp. 154–157.

[73] Mahsa Soufineyestani, Dale Dowling, and Arshia Khan. “Electroencephalography (EEG) Technology Applications and Available Devices”. In: *Applied Sciences* 10.21 (2020), p. 7453.

[74] Jerry J Shih, Dean J Krusienski, and Jonathan R Wolpaw. “Brain-computer interfaces in medicine”. In: *Mayo Clinic Proceedings*. Vol. 87. 3. Elsevier. 2012, pp. 268–279.

[75] JW Britton, LC Frey, and JL Hopp. *Introduction - Electroencephalography (EEG): An Introductory Text and Atlas of Normal and Abnormal Findings in Adults, Children, and Infants - NCBI Bookshelf*. Chicago, 2016. URL: https://www.ncbi.nlm.nih.gov/books/NBK390346/.

[76] *Invasive EEG Monitoring*. URL: https://my.clevelandclinic.org/health/diagnostics/17144-invasive-eeg-monitoring (visited on 01/20/2021).

[77] Maria Carolina Tigre Avelar. “Intellwheels–Controlling an Intelligent Wheelchair using a Brain Computer Interface”. PhD thesis. Universidade do Porto, 2019.

[78] Md Kafiul Islam, Amir Rastegarnia, and Zhi Yang. “Methods for artifact detection and removal from scalp EEG: A review”. In: *Neurophysiologie Clinique/Clinical Neurophysiology* 46.4-5 (2016), pp. 287–305.

[79] Khaled H. Jawabri and Sandeep Sharma. *Physiology, Cerebral Cortex Functions*. StatPearls Publishing, 2019. URL: http://www.ncbi.nlm.nih.gov/pubmed/30860731.

[80] *Cerebral Cortex - Neurology - Medbullets Step 1*. URL: https://step1.medbullets.com/neurology/113013/cerebral-cortex (visited on 01/20/2021).

[81] Mahtab Roohi-Azizi et al. “Changes of the brain’s bioelectrical activity in cognition, consciousness, and some mental disorders”. In: *Medical journal of the Islamic Republic of Iran* 31 (2017), p. 53.

[82] Erik Andreas Larsen. “Classification of EEG Signals in a Brain-Computer Interface System”. PhD thesis. Norwegian University of Science and Technology, 2011.

[83] Hayrettin Gürkök and Anton Nijholt. “Brain–computer interfaces for multimodal interaction: A survey and principles”. In: *International Journal of Human-Computer Interaction* 28.5 (2012), pp. 292–307.

[84] K Permana, SK Wijaya, and P Prajitno. “Controlled wheelchair based on brain computer interface using Neurosky Mindwave Mobile 2”. In: *AIP Conference Proceedings*. Vol. 2168. 1. AIP Publishing LLC. 2019, p. 020022.

[85] Mamunur Rashid et al. “Recent Trends and Open Challenges in EEG Based Brain-Computer Interface Systems”. In: *InECCE2019*. Springer, 2020, pp. 367–378.

[86] Adrienne Kline and Jaydip Desai. “SIMULINK® based robotic hand control using Emotiv™ EEG headset”. In: *2014 40th Annual Northeast Bioengineering Conference (NEBEC)*. IEEE. 2014, pp. 1–2.

[87] GN Ranky and S Adamovich. “Analysis of a commercial EEG device for the control of a robot arm”. In: *Proceedings of the 2010 IEEE 36th Annual Northeast Bioengineering Conference (NEBEC)*. IEEE. 2010, pp. 1–2.

[88] Yantao Li et al. “Towards an EEG-based brain-computer interface for online robot control”. In: *Multimedia Tools and Applications* 75.13 (2016), pp. 7999–8017.

[89] Ta-Tyonna Buck, Amber Matthews, and Rocio Alba-Flores. “Robotic Arm Control Through the Use of Human Machine Interfaces and Brain Signals”. In: *2019 SoutheastCon*. IEEE. 2019, pp. 1–4.

[90] Jozsef Katona et al. “Speed control of Festo Robotino mobile robot using NeuroSky MindWave EEG headset based brain-computer interface”. In: *2016 7th IEEE international conference on cognitive infocommunications (CogInfoCom)*. IEEE. 2016, pp. 000251–000256.

[91] Daniel Cernea et al. “Controlling in-vehicle systems with a commercial eeg headset: performance and cognitive load”. In: *Visualization of Large and Unstructured Data Sets: Applications in Geospatial Planning, Modeling and Engineering-Proceedings of IRTG 1131 Workshop 2011*. Schloss Dagstuhl-Leibniz-Zentrum für Informatik. 2012.

[92] SS Poorna et al. “Classification of EEG based control using ANN and KNN—A comparison”. In: *2016 IEEE International Conference on Computational Intelligence and Computing Research (ICCIC)*. IEEE. 2016, pp. 1–6.

[93] Daniel Göhring et al. “Semi-autonomous car control using brain computer interfaces”. In: *Intelligent Autonomous Systems 12*. Springer, 2013, pp. 393–408.

[94] Vinay Kumar Karigar Shivappa et al. “Home automation system using brain computer interface paradigm based on auditory selection attention”. In: *2018 IEEE International Instrumentation and Measurement Technology Conference (I2MTC)*. IEEE. 2018, pp. 1–6.

[95] Andrew Campbell et al. “NeuroPhone: brain-mobile phone interface using a wireless EEG headset”. In: *Proceedings of the second ACM SIGCOMM workshop on Networking, systems, and applications on mobile handhelds*. 2010, pp. 3–8.

[96] Krupal Sureshbai Mistry et al. “An SSVEP based brain computer interface system to control electric wheelchairs”. In: *2018 IEEE International Instrumentation and Measurement Technology Conference (I2MTC)*. IEEE. 2018, pp. 1–6.

[97] Agus Siswoyo, Zainal Arief, and Indra Adji Sulistijono. “Application of artificial neural networks in modeling direction wheelchairs using neurosky mindset mobile (EEG) device”. In: *EMITTER International Journal of Engineering Technology* 5.1 (2017), pp. 170–191.

[98] Imran Ali Mirza et al. “Mind-controlled wheelchair using an EEG headset and arduino microcontroller”. In: *2015 International Conference on Technologies for Sustainable Development (ICTSD)*. IEEE. 2015, pp. 1–5.

[99] Francesco Carrino et al. “A self-paced BCI system to control an electric wheelchair: Evaluation of a commercial, low-cost EEG device”. In: *2012 ISSNIP biosignals and biorobotics conference: biosignals and robotics for better and safer living (BRC)*. IEEE. 2012, pp. 1–6.

[100] Mohamad Amlie Abu Kasim et al. “User-friendly labview gui for prosthetic hand control using emotiv eeg headset”. In: *Procedia Computer Science* 105 (2017), pp. 276–281.

[101] Taha Beyrouthy et al. “EEG mind controlled smart prosthetic arm”. In: *2016 IEEE international conference on emerging technologies and innovative business practices for the transformation of societies (EmergiTech)*. IEEE. 2016, pp. 404–409.

[102] Martin Steinisch, Maria Gabriella Tana, and Silvia Comani. “A post-stroke rehabilitation system integrating robotics, VR and high-resolution EEG imaging”. In: *IEEE Transactions on Neural Systems and Rehabilitation Engineering* 21.5 (2013), pp. 849–859.

[103] Tong Jijun et al. “The portable P300 dialing system based on tablet and Emotiv Epoc headset”. In: *2015 37th Annual International Conference of the IEEE Engineering in Medicine and Biology Society (EMBC)*. IEEE. 2015, pp. 566–569.

[104] James Derek Jacoby, Melanie Tory, and James Tanaka. “Evoked response potential training on a consumer EEG headset”. In: *2015 IEEE Pacific Rim Conference on Communications, Computers and Signal Processing (PACRIM)*. IEEE. 2015, pp. 485–490.

[105] Mohammad H Alomari et al. “EEG mouse: A machine learning-based brain computer interface”. In: *Int. J. Adv. Comput. Sci. Appl* 5.4 (2014), pp. 193–198.

[106] Fabio Aloise et al. “Asynchronous gaze-independent event-related potential-based brain–computer interface”. In: *Artificial intelligence in medicine* 59.2 (2013), pp. 61–69.

[107] Omamah Hawsawi and Sudhanshu K Semwal. “EEG headset supporting mobility impaired gamers with game accessibility”. In: *2014 IEEE International Conference on Systems, Man, and Cybernetics (SMC)*. IEEE. 2014, pp. 837–841.

[108] Rain Ashford. “ThinkerBelle EEG amplifying dress”. In: *Adjunct Proceedings of the 2015 ACM International Joint Conference on Pervasive and Ubiquitous Computing and Proceedings of the 2015 ACM International Symposium on Wearable Computers*. 2015, pp. 607–612.

[109] John LaRocco, Minh Dong Le, and Dong-Guk Paeng. “A systemic review of available low-cost EEG headsets used for drowsiness detection”. In: *Frontiers in neuroinformatics* 14 (2020).

[110] *MindWave*. URL: https://store.neurosky.com/pages/mindwave (visited on 01/21/2021).

[111] *Muse 2: Brain Sensing Headband - Technology Enhanced Meditation*. URL: https://choosemuse.com/muse-2/ (visited on 01/21/2021).

[112] *Ultracortex "Mark IV" EEG Headset – OpenBCI Online Store*. URL: https://shop.openbci.com/collections/frontpage/products/ultracortex-mark-iv?variant=43568381966 (visited on 01/21/2021).

[113] *EMOTIV EPOC X 14 Channel Mobile Brainwear® | EMOTIV*. URL: https://www.emotiv.com/product/emotiv-epoc-x-14-channel-mobile-brainwear/ (visited on 01/21/2021).

[114] *MindWave Mobile 2 Transition Doc*. Tech. rep. 2018.

[115] Swati Banerjee and Rajdeep Chatterjee. "Temporal Window based Feature Extraction Technique for Motor-Imagery EEG Signal Classification". In: *bioRxiv* (2021).

[116] Ali Boyali, Naohisa Hashimoto, and Manolya Kavakli. "Continuous and Simultaneous Gesture and Posture Recognition for Commanding a Robotic Wheelchair; Towards Spotting the Signal Patterns". In: *arXiv preprint arXiv:1512.00622* (2015).

[117] Mohamed Mohandes, S Aliyu, and Mohamed Deriche. "Prototype Arabic Sign language recognition using multi-sensor data fusion of two leap motion controllers". In: *2015 IEEE 12th International Multi-Conference on Systems, Signals & Devices (SSD15)*. IEEE. 2015, pp. 1–6.

[118] Romy Budhi Widodo et al. "A study of hand-movement gestures to substitute for mouse-cursor placement using an inertial sensor". In: *Journal of Sensors and Sensor Systems* 8.1 (2019), pp. 95–104.

[119] Ranathunga Arachchilage Ruwan Chandra Gopura and Kazuo Kiguchi. "An exoskeleton robot for human forearm and wrist motion assist-hardware design and EMG-based controller". In: *Journal of Advanced Mechanical Design, Systems, and Manufacturing* 2.6 (2008), pp. 1067–1083.

[120] Laurens Van Der Maaten, Eric Postma, and Jaap Van den Herik. "Dimensionality reduction: a comparative". In: *J Mach Learn Res* 10.66-71 (2009), p. 13.

[121] Varsha Harpale and Vinayak Bairagi. "An adaptive method for feature selection and extraction for classification of epileptic EEG signal in significant states". In: *Journal of King Saud University-Computer and Information Sciences* (2018).

[122] J.E. Tomaszewski et al. "Machine Vision and Machine Learning in Digital Pathology". In: *Pathobiology of Human Disease*. Ed. by Linda M. McManus and Richard N. Mitchell. San Diego: Academic Press, 2014, pp. 3711–3722. ISBN: 978-0-12-386457-4. DOI: https://doi.org/10.1016/B978-0-12-386456-7.07202-6. URL: https://www.sciencedirect.com/science/article/pii/B9780123864567072026.

[123] *Classification: Precision and Recall | Machine Learning Crash Course*. URL: https://developers.google.com/machine-learning/crash-course/classification/precision-and-recall (visited on 06/08/2021).

[124] Ekaba Bisong. *Building Machine Learning and Deep Learning Models on Google Cloud Platform: A Comprehensive Guide for Beginners*. Apress, 2019.

[125] Zhongheng Zhang. "Naïve Bayes classification in R". In: *Annals of translational medicine* 4.12 (2016).

[126] Rajeev DS Raizada and Yune-Sang Lee. "Smoothness without smoothing: why Gaussian naive Bayes is not naive for multi-subject searchlight studies". In: *PloS one* 8.7 (2013), e69566.

[127] *K-Nearest Neighbor (K-NN) - Definition from Techopedia*. URL: https://www.techopedia.com/definition/32066/k-nearest-neighbor-k-nn (visited on 06/08/2021).

[128] Valentina Emilia Balas, Vijender Kumar Solanki, and Raghvendra Kumar. *An Industrial IoT Approach for Pharmaceutical Industry Growth: Volume 2*. Academic Press, 2020.

[129] *Classification: Precision and Recall | Machine Learning Crash Course*. URL: https://developers.google.com/machine-learning/crash-course/classification/precision-and-recall (visited on 06/08/2021).

[130] Anita Rácz, Dávid Bajusz, and Károly Héberger. "Multi-level comparison of machine learning classifiers and their performance metrics". In: *Molecules* 24.15 (2019), p. 2811.

[131] *ML - Support Vector Machine(SVM) - Tutorialspoint*. URL: https://www.tutorialspoint.com/machine_learning_with_python/machine_learning_with_python_classification_algorithms_support_vector_machine.htm (visited on 06/09/2021).

[132] *1.17. Neural network models (supervised) — scikit-learn 0.24.2 documentation*. URL: https://scikit-learn.org/stable/modules/neural_networks_supervised.html (visited on 06/10/2021).

[133] *Understanding Backpropagation Algorithm | by Simeon Kostadinov | Towards Data Science*. URL: https://towardsdatascience.com/understanding-backpropagation-algorithm-7bb3aa2f95fd (visited on 06/10/2021).

[134] *Ensemble Machine Learning Algorithms in Python with scikit-learn*. URL: https://machinelearningmastery.com/ensemble-machine-learning-algorithms-python-scikit-learn/ (visited on 06/10/2021).

[135] *AdaBoost Algorithm: Boosting Algorithm in Machine Learning*. URL: https://www.mygreatlearning.com/blog/adaboost-algorithm/ (visited on 06/10/2021).

[136] R Leeb et al. "BCI Competition 2008–Graz data set B". In: *Graz University of Technology, Austria* (2008), pp. 1–6.

[137] Arjon Turnip et al. "EEG-based brain-controlled wheelchair with four different stimuli frequencies". In: *Internetworking Indonesia Journal* 8.1 (2016), pp. 65–69.

[138] Matteo Fraschini et al. "The effect of epoch length on estimated EEG functional connectivity and brain network organisation". In: *Journal of neural engineering* 13.3 (2016), p. 036015.

[139] Rab Nawaz et al. "Comparison of different feature extraction methods for EEG-based emotion recognition". In: *Biocybernetics and Biomedical Engineering* 40.3 (2020), pp. 910–926.

[140] Fanny Monori and Stefan Oniga. “Processing EEG signals acquired from a consumer grade BCI device”. In: *Carpathian Journal of Electronic and Computer Engineering* 11.2 (2018), pp. 29–34.

[141] Jozsef Suto and Stefan Oniga. “Efficiency investigation of artificial neural networks in human activity recognition”. In: *Journal of Ambient Intelligence and Humanized Computing* 9.4 (2018), pp. 1049–1060.

[142] Na Ji et al. “EEG signals feature extraction based on DWT and EMD combined with approximate entropy”. In: *Brain sciences* 9.8 (2019), p. 201.

[143] Syed Khairul Bashar and Mohammed Imamul Hassan Bhuiyan. “Classification of motor imagery movements using multivariate empirical mode decomposition and short time Fourier transform based hybrid method”. In: *Engineering science and technology, an international journal* 19.3 (2016), pp. 1457–1464.

[144] Natasha Padfield et al. “EEG-based brain-computer interfaces using motor-imagery: Techniques and challenges”. In: *Sensors* 19.6 (2019), p. 1423.

[145] Piyush Kant, Jupitara Hazarika, and SH Laskar. “Wavelet transform based approach for EEG feature selection of motor imagery data for braincomputer interfaces”. In: *2019 Third International Conference on Inventive Systems and Control (ICISC)*. IEEE. 2019, pp. 101–105.

[146] Fanny Monori and Stefan Oniga. “Processing EEG signals acquired from a consumer grade BCI device”. In: *Carpathian Journal of Electronic and Computer Engineering* 11.2 (2018), pp. 29–34. DOI: doi:10.2478/cjece-2018-0015. URL: https://doi.org/10.2478/cjece-2018-0015.

[147] Seung-Hyeon Oh, Yu-Ri Lee, and Hyoung-Nam Kim. “A novel EEG feature extraction method using Hjorth parameter”. In: *International Journal of Electronics and Electrical Engineering* 2.2 (2014), pp. 106–110.

[148] E Olofsen, JW Sleigh, and A Dahan. “Permutation entropy of the electroencephalogram: a measure of anaesthetic drug effect”. In: *British journal of anaesthesia* 101.6 (2008), pp. 810–821.

[149] Jörgen Bruhn, Heiko Röpcke, and Andreas Hoeft. “Approximate entropy as an electroencephalographic measure of anesthetic drug effect during desflurane anesthesia”. In: *The Journal of the American Society of Anesthesiologists* 92.3 (2000), pp. 715–726.

[150] Rosana Esteller et al. “A comparison of waveform fractal dimension algorithms”. In: *IEEE Transactions on Circuits and Systems I: Fundamental Theory and Applications* 48.2 (2001), pp. 177–183.

[151] Arthur Petrosian. “Kolmogorov complexity of finite sequences and recognition of different preictal EEG patterns”. In: *Proceedings eighth IEEE symposium on computer-based medical systems*. IEEE. 1995, pp. 212–217.

[152] Tomoyuki Higuchi. “Approach to an irregular time series on the basis of the fractal theory”. In: *Physica D: Nonlinear Phenomena* 31.2 (1988), pp. 277–283.

[153] Beatriz García-Martínez et al. “A review on nonlinear methods using electroencephalographic recordings for emotion recognition”. In: *IEEE Transactions on Affective Computing* (2019).

[154] Norden E Huang et al. “The empirical mode decomposition and the Hilbert spectrum for nonlinear and non-stationary time series analysis”. In: *Proceedings of the Royal Society of London. Series A: mathematical, physical and engineering sciences* 454.1971 (1998), pp. 903–995.

[155] K Permana, SK Wijaya, and P Prajitno. “Controlled wheelchair based on brain computer interface using Neurosky Mindwave Mobile 2”. In: *AIP Conference Proceedings*. Vol. 2168. 1. AIP Publishing LLC. 2019, p. 020022.

Appendix A

Informed Consent

CONSENTIMENTO INFORMADO, LIVRE E ESCLARECIDO PARA PARTICIPAÇÃO EM INVESTIGAÇÃO

Conforme a lei 67/98 de 26 de Outubro e a "Declaração de Helsínquia" da Associação Médica Mundial (Helsínquia 1964; Tóquio 1975; Veneza 1983; Hong Kong 1989; Somerset West 1996, Edimburgo 2000; Washington 2002, Tóquio 2004, Seul 2008)

Designação do Estudo: IntellWheels2.0 – Cadeira de Rodas Inteligente com Interface Multimodal Flexível e Simulador Realista

Consórcio: Laboratório de Inteligência Artificial e Ciência de Computadores (LIACC) da Faculdade de Engenharia da Universidade do Porto, Optimizer - Serviços e Consultoria Informática Lda, Instituto de Engenharia Eletrónica e Telemática de Aveiro (IEETA) da Universidade de Aveiro, Ground Control Studios (GCS) e RehaPoint.

Fui informado(a) de que o Estudo de Investigação acima mencionado se destina a obter dados sobre o desempenho na condução de uma cadeira de rodas inteligente (CRI) recorrendo a uma interface multimodal. Esta interface permite conduzir a CRI utilizando diversos inputs, tais como: movimentos de cabeça, comandos de voz, através de uma *brain computer interface*, *gamepad* e *joystick*.

Fui ainda informado(a) que neste estudo está prevista a realização de testes utilizando o sensor *NeuroSky MindWave Mobile 2* e o preenchimento de questionários tendo-me sido explicado em que consistem e quais os seus possíveis efeitos.

Foi-me garantido que todos os dados relativos à identificação dos Participantes neste estudo são confidenciais e que será mantido o anonimato.

Sei que posso recusar participar ou interromper a qualquer momento a participação no estudo, sem nenhum tipo de penalização.

Fui informado(a) de que não está contemplado qualquer ressarcimento ou remuneração para participação no estudo assim como não apresenta qualquer custo para os participantes.

Compreendi a informação que me foi dada, tive oportunidade de fazer perguntas e as minhas dúvidas foram esclarecidas.

Em nome da equipa agradecemos a sua participação.

Investigador responsável: Professor Doutor Luís Paulo Reis

Assinatura: … … … … … … … … … … … … … … … … ..... … … … … … … … … … … … … … …

-o-o-o-o-o-o-o-o-o-o-o-o-o-o-o-o-o-o-o-o-o-

Eu, abaixo-assinado aceito participar de livre vontade no estudo acima mencionado. Também autorizo a divulgação dos resultados obtidos no meio científico, com as garantias de anonimato e confidencialidade dos dados fornecidos.

Data Assinatura

Nome do investigador responsável e contacto: Luís Paulo Reis (lpreis@fe.up.pt)

… … /… … /… … ……

Se não for o participante do estudo a assinar:

Eu, abaixo-assinado _____(nome completo do representante legal do participante do estudo), na qualidade de representante legal de _____ (nome completo do participante do estudo) autorizo de livre vontade a participação daquele que legalmente represento no estudo acima mencionado.

Data Assinatura

… … /… … /… … ……

ESTE DOCUMENTO É COMPOSTO POR 2 PÁGINAS E FEITO EM DUPLICADO: UMA VIA VAI PARA O/A INVESTIGADOR/A, OUTRA PARA A PESSOA QUE CONSENTE.

Nome do investigador responsável e contacto: Luís Paulo Reis (lpreis@fe.up.pt)

Appendix B

Results for each classifier

B.1 Leap Motion

Table B.1: Results of each classifier obtained on the Leap Motion Data Set.

Classifier	GaussianNB			SVM			DTC			RF			KNN			LR			LDA			LSVM			MLP		
Feature Scaling	-	Stand	Norm	-	Stand	Norm	-	Stand	Norm	-	Stand	Norm	-	Stand	Norm	-	Stand	Norm	-	Stand	Norm	-	Stand	Norm	-	Stand	Norm
1	0,65	0,98	0,50	0,82	1,00	0,84	0,84	1,00	0,76	0,85	1,00	0,83	0,81	1,00	0,70	0,74	0,99	0,78	0,78	0,99	0,81	0,78	0,99	0,49	0,83	1,00	0,84
2	0,96	0,93	0,63	0,97	0,99	0,85	0,98	0,97	0,65	0,98	0,98	0,77	0,96	0,98	0,60	0,97	0,93	0,81	0,97	0,97	0,82	0,60	0,94	0,43	0,98	0,99	0,84
3	0,28	0,97	0,70	0,50	0,98	0,66	0,50	0,98	0,62	0,50	0,99	0,68	0,44	0,98	0,67	0,31	0,96	0,66	0,31	0,97	0,66	0,34	0,93	0,36	0,52	0,99	0,66
4	0,33	0,95	0,79	0,52	0,98	0,73	0,49	0,98	0,66	0,49	0,98	0,69	0,43	0,97	0,67	0,28	0,95	0,71	0,29	0,95	0,75	0,32	0,92	0,35	0,51	0,98	0,63
5	0,33	0,95	0,83	0,52	0,97	0,87	0,50	0,97	0,74	0,50	0,97	0,78	0,43	0,96	0,74	0,29	0,96	0,86	0,29	0,95	0,87	0,22	0,93	0,40	0,53	0,97	0,88

B.2 NeuroSky Mindwave Mobile 2

Table B.2: Results of each classifier obtained on Data Set A with an epoch of 4s.

Dataset A (epoch 4s)																											
Classifier	GaussianNB			SVM			DTC			RF			KNN			LR			LDA			LSVM			MLP		
Feature Scaling	-	Stand	Norm	-	Stand	Norm	-	Stand	Norm	-	Stand	Norm	-	Stand	Norm	-	Stand	Norm	-	Stand	Norm	-	Stand	Norm	-	Stand	Norm
1	0,56	0,17	0,17	0,56	0,56	0,22	0,22	1,00	0,17	0,56	0,56	0,33	0,17	0,56	0,33	0,56	1,00	0,56	0,56	1,00	0,33	0,56	1,00	0,56	0,56	1,00	0,56
2	0,00	0,44	0,00	0,00	0,67	0,00	0,44	1,00	0,00	0,44	1,00	0,00	0,00	0,44	0,00	0,00	0,44	0,00	0,44	0,67	0,00	0,44	0,67	0,00	0,44	1,00	0,00
3	0,33	0,78	0,33	0,00	0,00	0,53	0,00	0,67	0,53	0,00	0,33	0,53	0,44	0,00	0,53	0,00	0,00	0,53	0,00	0,33	0,00	0,00	0,00	0,53	0,00	0,44	0,53
4	0,00	0,67	0,44	0,44	1,00	0,67	0,78	0,00	0,00	0,33	0,00	0,44	0,44	0,78	0,00	0,78	1,00	0,44	0,78	0,78	0,67	0,78	0,78	0,44	0,78	1,00	0,44
5	0,33	0,78	0,00	0,22	0,78	0,00	0,53	0,78	0,00	0,33	0,78	0,00	0,33	0,78	0,00	0,22	0,33	0,00	0,67	0,78	0,00	0,17	0,78	0,00	0,00	0,78	0,00
6	0,22	1,00	0,67	0,17	0,17	0,00	0,17	1,00	0,67	0,22	1,00	0,67	0,22	0,67	0,00	0,67	1,00	0,00	0,67	1,00	0,44	0,22	1,00	0,67	0,22	1,00	0,00
7	1,00	0,67	0,00	0,00	1,00	0,00	0,33	0,17	0,44	0,17	0,67	0,44	0,00	0,67	0,44	1,00	0,67	0,44	1,00	1,00	0,44	0,00	1,00	0,44	1,00	1,00	0,00
8	0,22	0,22	0,00	0,22	0,22	0,22	0,00	0,22	0,22	0,67	0,22	0,22	0,44	0,00	0,33	0,22	0,22	0,22	0,00	0,00	0,22	0,22	0,22	0,22	0,22	0,44	0,22
9	0,00	0,44	0,44	0,00	1,00	0,00	0,00	1,00	0,44	0,44	1,00	0,44	0,00	0,67	0,00	0,00	1,00	0,00	0,44	1,00	0,33	0,78	1,00	0,44	0,44	1,00	0,22
10	0,00	0,22	0,17	0,33	0,33	0,67	0,00	0,22	0,33	0,44	0,22	0,67	0,33	0,78	0,00	0,00	0,78	0,00	0,00	0,78	0,67	0,00	0,33	0,17	0,00	0,33	0,17
11	0,67	0,78	0,00	0,00	0,17	0,00	0,67	0,53	0,00	0,67	0,53	0,00	0,17	0,67	0,00	0,67	0,53	0,00	0,22	1,00	0,00	0,67	0,53	0,00	0,22	0,53	0,00
12	0,00	0,00	0,33	0,00	1,00	0,33	0,00	0,78	0,33	0,33	1,00	0,33	0,44	0,53	0,33	0,00	1,00	0,33	0,00	1,00	0,33	0,44	1,00	0,33	0,33	1,00	0,33

Table B.3: Results of each classifier obtained on Data Set A with an epoch of 3s.

Dataset A (epoch 3s)																								
Classifier	GaussianNB			SVM			DTC			RF			KNN			LR			LDA			LSVM			MLP		
Feature Scaling	-	Stand	Norm	-	Stand	Norm	-	Stand	Norm	-	Stand	Norm	-	Stand	Norm	-	Stand	Norm	-	Stand	Norm	-	Stand	Norm	-	Stand	Norm
1	0,54	0,30	0,00	0,17	0,50	0,17	0,50	0,64	0,17	0,77	0,64	0,00	0,30	0,64	0,00	0,13	0,64	0,00	0,54	0,64	0,00	0,60	0,75	0,00	0,77	0,64	0,00
2	0,25	0,38	0,00	0,00	0,85	0,00	0,00	0,63	0,38	0,63	0,38	0,38	0,17	0,63	0,00	0,77	0,85	0,00	0,60	0,85	0,38	0,77	0,25	0,00	0,38	0,85	0,00
3	0,38	0,38	0,00	0,00	0,17	0,00	0,00	0,38	0,00	0,38	0,00	0,00	0,00	0,63	0,17	0,00	0,63	0,17	0,00	0,25	0,25	0,00	0,63	0,17	0,00	0,25	0,17
4	0,00	0,00	0,60	0,00	0,38	0,00	0,38	0,38	0,60	0,38	0,38	0,75	0,00	0,38	0,17	0,38	0,75	0,75	0,60	0,60	0,75	0,00	0,60	0,60	0,00	0,60	0,60
5	0,50	0,13	0,10	0,00	0,30	0,10	0,00	0,30	0,50	0,00	0,30	0,00	0,00	0,50	0,10	0,00	0,50	0,10	0,00	0,50	0,13	0,30	0,50	0,10	0,00	0,50	0,10
6	0,64	0,50	0,00	0,00	0,85	0,63	0,50	0,50	0,38	0,50	0,60	0,00	0,00	0,54	0,38	0,00	0,64	0,38	0,30	0,50	0,38	0,50	0,50	0,38	0,30	0,64	0,38
7	0,00	0,54	0,00	0,00	0,17	0,13	0,38	0,30	0,13	0,00	0,38	0,00	0,00	0,30	0,13	0,38	0,54	0,13	0,00	0,17	0,13	0,10	0,54	0,13	0,38	0,54	0,13
8	0,38	0,75	0,38	0,00	0,00	0,60	0,75	0,60	0,54	0,60	0,75	0,54	0,50	0,64	0,38	0,00	0,60	0,38	0,75	0,75	0,60	0,38	0,60	0,38	0,00	0,75	0,38
9	0,17	0,60	0,00	0,00	0,00	0,00	0,77	0,60	0,75	0,60	0,60	0,00	0,77	0,77	0,60	0,60	0,75	0,75	0,77	0,60	0,60	0,00	0,75	0,60	0,00	0,60	0,75
10	0,17	0,25	0,00	0,17	0,60	0,13	0,17	0,77	0,10	0,17	1,00	0,13	0,13	0,10	0,10	0,63	0,75	0,00	0,63	0,60	0,10	0,25	0,75	0,13	0,17	0,60	0,00
11	0,00	0,25	0,00	0,00	0,64	0,13	0,63	0,38	0,13	0,60	0,64	0,54	0,38	0,64	0,13	0,60	0,63	0,13	0,38	0,64	0,13	0,50	0,64	0,13	0,50	0,64	0,13
12	1,00	0,38	0,00	0,00	0,00	0,00	0,60	0,00	0,10	0,60	0,38	0,13	0,17	0,00	0,00	0,00	0,10	0,00	0,00	0,00	0,00	0,00	0,10	0,00	0,00	0,10	0,00

Table B.4: Results of each classifier obtained on Data Set A with an epoch of 2s.

Dataset A (epoch 2s)																								
Classifier	GaussianNB			SVM			DTC			RF			KNN			LR			LDA			LSVM			MLP		
Feature Scaling	-	Stand	Norm	-	Stand	Norm	-	Stand	Norm	-	Stand	Norm	-	Stand	Norm	-	Stand	Norm	-	Stand	Norm	-	Stand	Norm	-	Stand	Norm
1	0,64	0,60	0,11	0,25	0,43	0,08	0,79	0,50	0,11	0,79	0,54	0,07	0,67	0,54	0,22	0,54	0,54	0,11	0,51	0,11	0,44	0,54	0,36	0,42	0,65	0,50	0,11
2	0,52	0,33	0,13	1,00	0,28	0,57	0,42	0,54	0,40	0,57	0,57	0,40	0,83	0,54	0,50	0,51	0,54	0,40	0,63	0,82	0,40	0,51	0,60	0,25	0,42	0,54	0,33
3	0,19	0,19	0,04	0,10	0,38	0,26	0,21	0,10	0,26	0,29	0,10	0,24	0,10	0,40	0,29	0,16	0,31	0,16	0,29	0,29	0,26	0,16	0,29	0,16	0,17	0,29	0,00
4	0,00	0,33	0,57	0,00	0,22	0,13	0,62	0,42	0,13	0,50	0,56	0,42	0,20	0,25	0,38	0,00	0,52	0,13	0,50	0,47	0,11	0,20	0,22	0,13	0,00	0,22	0,13
5	0,08	0,62	0,48	0,07	0,27	0,40	0,00	0,57	0,38	0,00	0,67	0,40	0,25	0,67	0,57	0,40	0,62	0,40	0,47	0,62	0,51	0,06	0,62	0,40	0,22	0,67	0,40
6	0,00	0,25	0,33	0,08	0,25	0,17	0,00	0,00	0,17	0,00	0,22	0,00	0,00	0,47	0,00	0,00	0,00	0,11	0,08	0,00	0,19	0,22	0,00	0,00	0,00	0,25	0,11
7	0,17	0,36	0,20	0,10	0,13	0,33	0,11	0,28	0,50	0,10	0,28	0,42	0,38	0,42	0,33	0,36	0,36	0,33	0,11	0,64	0,33	0,36	0,36	0,42	0,25	0,28	0,33
8	0,31	0,31	0,40	0,00	0,69	0,00	0,00	0,44	0,13	0,23	0,33	0,22	0,00	0,64	0,33	0,35	0,84	0,35	0,31	0,56	0,35	0,11	0,56	0,35	0,27	0,56	0,35
9	0,32	0,51	0,25	0,48	0,42	0,36	0,36	0,68	0,40	0,48	0,71	0,25	0,31	0,42	0,51	0,48	0,54	0,36	0,48	0,71	0,51	0,48	0,42	0,11	0,33	0,44	0,33
10	0,47	0,56	0,48	0,00	0,40	0,50	0,00	0,53	0,13	0,00	0,57	0,42	0,47	0,57	0,42	0,25	0,62	0,50	0,25	0,56	0,50	0,29	0,71	0,50	0,20	0,57	0,50
11	0,50	0,23	0,40	0,08	0,37	0,40	0,28	0,50	0,47	0,50	0,53	0,25	0,28	0,50	0,43	0,23	0,50	0,51	0,50	0,68	0,61	0,50	0,50	0,51	0,56	0,17	0,51
12	0,05	0,00	0,50	0,00	0,00	0,42	0,19	0,40	0,17	0,00	0,00	0,17	0,28	0,68	0,33	0,05	0,68	0,17	0,05	0,17	0,56	0,33	0,17	0,50	0,00	0,27	0,17

Table B.5: Results of each classifier obtained on Data Set B with an epoch of 4s.

Dataset B (epoch 4s)																								
Classifier	GaussianNB			SVM			DTC			RF			KNN			LR			LDA			LSVM			MLP		
Feature Scaling	-	Stand	Norm	-	Stand	Norm	-	Stand	Norm	-	Stand	Norm	-	Stand	Norm	-	Stand	Norm	-	Stand	Norm	-	Stand	Norm	-	Stand	Norm
1	0,60	0,60	0,10	0,81	0,57	0,27	0,58	0,57	0,07	0,81	0,60	0,27	0,60	0,81	0,38	0,71	0,60	0,57	0,60	0,60	0,28	0,81	0,60	0,38	0,60	0,60	0,13
2	0,13	0,58	0,40	0,00	0,61	0,50	0,30	0,61	0,00	0,00	0,61	0,43	0,24	0,58	0,50	0,08	0,61	0,43	0,08	0,38	0,30	0,00	0,58	0,43	0,00	0,58	0,50
3	0,53	0,61	0,43	0,34	0,61	0,61	0,20	0,61	0,68	0,34	0,61	0,61	0,53	0,73	0,61	0,71	0,73	0,61	0,53	0,43	0,61	0,24	0,73	0,73	0,34	0,73	0,61
4	0,81	0,08	0,13	0,61	0,08	0,13	0,81	0,38	0,13	0,63	0,08	0,13	0,40	0,60	0,40	0,38	0,08	0,13	0,38	0,38	0,40	0,38	0,08	0,13	0,38	0,63	0,13
5																											
6	0,73	0,43	0,80	0,58	0,61	0,73	0,88	0,60	0,80	0,43	0,61	0,80	0,34	0,60	0,73	0,73	0,61	0,73	0,80	0,61	0,73	0,73	0,81	0,73	0,73	0,61	0,61
7	0,30	0,48	0,08	0,30	0,61	0,07	0,00	0,61	0,10	0,00	0,61	0,10	0,48	0,53	0,08	0,10	0,48	0,07	0,00	0,61	0,08	0,40	0,60	0,10	0,40	0,60	0,07
8	0,34	0,44	0,00	0,07	0,44	0,00	0,38	0,58	0,00	0,10	0,43	0,00	0,24	0,44	0,00	0,23	0,10	0,00	0,08	0,44	0,00	0,30	0,44	0,00	0,60	0,44	0,00
9	0,40	0,08	0,07	0,40	0,00	0,07	0,00	0,10	0,08	0,00	0,00	0,08	0,30	0,40	0,30	0,30	0,00	0,00	0,43	0,00	0,00	0,10	0,24	0,00	0,10	0,00	0,07
10	0,13	0,60	0,43	0,57	0,43	0,81	0,57	0,80	0,37	0,57	0,63	0,88	0,53	0,80	0,40	0,37	0,43	0,23	0,60	0,63	0,71	0,63	0,63	0,23	0,63	0,63	0,63
11	0,61	0,40	0,23	0,07	0,24	0,34	0,53	0,00	0,53	0,63	0,00	0,53	0,43	0,40	0,13	0,71	0,24	0,34	0,07	0,00	0,34	0,61	0,00	0,08	0,20	0,24	0,08
12	0,53	0,00	0,30	0,07	0,81	0,30	0,53	0,68	0,51	0,53	0,58	0,48	0,45	0,73	0,68	0,43	0,70	0,48	0,58	0,63	0,30	0,30	0,70	0,48	0,61	0,88	0,48

Table B.6: Results of each classifier obtained on Data Set B with an epoch of 3s.

Dataset B (epoch 3s)																								
Classifier	GaussianNB			SVM			DTC			RF			KNN			LR			LDA			LSVM			MLP		
Feature Scaling	-	Stand	Norm	-	Stand	Norm	-	Stand	Norm	-	Stand	Norm	-	Stand	Norm	-	Stand	Norm	-	Stand	Norm	-	Stand	Norm	-	Stand	Norm
1	0,33	0,48	0,13	0,00	0,44	0,13	0,00	0,10	0,00	0,21	0,18	0,00	0,08	0,29	0,00	0,08	0,10	0,13	0,21	0,06	0,00	0,08	0,06	0,13	0,00	0,39	0,13
2	0,72	0,51	0,00	0,17	0,35	0,00	0,44	0,63	0,00	0,22	0,38	0,00	0,25	0,33	0,13	0,67	0,35	0,00	0,72	0,43	0,00	0,16	0,43	0,00	0,48	0,43	0,00
3	0,00	0,61	0,38	0,08	0,00	0,20	0,08	0,00	0,00	0,08	0,00	0,00	0,10	0,08	0,14	0,30	0,30	0,17	0,35	0,38	0,25	0,44	0,38	0,17	0,18	0,38	0,20
4	0,10	0,08	0,13	0,08	0,10	0,08	0,31	0,59	0,25	0,08	0,00	0,31	0,07	0,23	0,08	0,13	0,21	0,14	0,10	0,10	0,08	0,13	0,25	0,14	0,13	0,15	0,14
5																											
6	0,00	0,36	0,04	0,00	0,00	0,00	0,00	0,07	0,00	0,00	0,58	0,00	0,00	0,27	0,00	0,00	0,07	0,00	0,08	0,00	0,04	0,10	0,10	0,00	0,31	0,31	0,00
7	0,19	0,38	0,00	0,13	0,20	0,56	0,17	0,41	0,00	0,26	0,33	0,21	0,13	0,17	0,00	0,26	0,41	0,00	0,26	0,38	0,47	0,26	0,41	0,00	0,47	0,38	0,21
8	0,00	0,24	0,04	0,03	0,07	0,00	0,03	0,08	0,03	0,03	0,08	0,00	0,10	0,08	0,00	0,00	0,06	0,00	0,03	0,10	0,00	0,10	0,10	0,00	0,00	0,06	0,00
9	0,23	0,28	0,00	0,13	0,20	0,00	0,00	0,20	0,21	0,00	0,20	0,00	0,17	0,20	0,00	0,10	0,17	0,00	0,31	0,20	0,00	0,06	0,20	0,00	0,13	0,20	0,00
10	0,29	0,35	0,00	0,18	0,17	0,00	0,00	0,00	0,00	0,21	0,00	0,00	0,13	0,07	0,13	0,11	0,03	0,00	0,10	0,17	0,04	0,08	0,13	0,00	0,31	0,00	0,00
11	0,20	0,33	0,17	0,00	0,06	0,21	0,38	0,08	0,31	0,50	0,29	0,21	0,13	0,15	0,17	0,10	0,58	0,21	0,38	0,67	0,52	0,00	0,75	0,21	0,07	0,27	0,29
12	0,05	0,17	0,00	0,06	0,21	0,00	0,33	0,18	0,00	0,10	0,21	0,00	0,29	0,06	0,10	0,08	0,23	0,00	0,06	0,08	0,31	0,06	0,18	0,00	0,00	0,23	0,00

Table B.7: Results of each classifier obtained on Data Set B with an epoch of 2s.

Dataset B (epoch 2s)																									
Classifier	GaussianNB			SVM			DTC			RF			KNN			LR			LDA			LSVM			MLP		
Feature Scaling	-	Stand	Norm	-	Stand	Norm	-	Stand	Norm	-	Stand	Norm	-	Stand	Norm	-	Stand	Norm	-	Stand	Norm	-	Stand	Norm	-	Stand	Norm
1	0,22	0,34	0,17	0,30	0,33	0,24	0,21	0,17	0,17	0,00	0,11	0,17	0,29	0,06	0,14	0,28	0,19	0,17	0,23	0,08	0,17	0,29	0,09	0,17	0,41	0,00	0,10
2	0,19	0,35	0,17	0,19	0,35	0,33	0,15	0,26	0,15	0,34	0,50	0,29	0,25	0,38	0,21	0,24	0,47	0,30	0,00	0,34	0,43	0,10	0,48	0,30	0,23	0,33	0,30
3	0,35	0,34	0,08	0,31	0,11	0,06	0,35	0,37	0,25	0,23	0,38	0,08	0,21	0,27	0,05	0,38	0,22	0,08	0,27	0,24	0,08	0,15	0,23	0,07	0,23	0,39	0,08
4	0,16	0,13	0,17	0,15	0,29	0,44	0,33	0,42	0,46	0,24	0,68	0,30	0,00	0,30	0,31	0,13	0,41	0,17	0,18	0,24	0,30	0,12	0,29	0,30	0,10	0,36	0,32
5																											
6	0,33	0,34	0,10	0,23	0,38	0,18	0,33	0,30	0,12	0,28	0,36	0,18	0,23	0,27	0,22	0,32	0,43	0,23	0,33	0,37	0,37	0,25	0,67	0,23	0,21	0,38	0,23
7	0,49	0,40	0,17	0,10	0,49	0,13	0,25	0,30	0,17	0,33	0,48	0,17	0,33	0,37	0,14	0,53	0,41	0,17	0,22	0,44	0,17	0,11	0,57	0,17	0,42	0,68	0,17
8	0,32	0,27	0,06	0,25	0,10	0,08	0,13	0,26	0,10	0,12	0,43	0,05	0,10	0,23	0,08	0,44	0,28	0,07	0,44	0,11	0,07	0,38	0,28	0,07	0,47	0,13	0,14
9	0,39	0,33	0,29	0,28	0,42	0,36	0,15	0,21	0,29	0,25	0,32	0,29	0,28	0,42	0,29	0,49	0,35	0,29	0,37	0,18	0,24	0,16	0,29	0,29	0,28	0,49	0,23
10	0,62	0,50	0,12	0,60	0,40	0,15	0,52	0,32	0,11	0,50	0,46	0,12	0,39	0,39	0,24	0,80	0,47	0,12	0,60	0,40	0,23	0,62	0,47	0,12	0,60	0,49	0,45
11	0,16	0,25	0,07	0,12	0,10	0,31	0,25	0,14	0,07	0,24	0,16	0,07	0,30	0,18	0,38	0,35	0,46	0,22	0,25	0,39	0,22	0,17	0,47	0,22	0,24	0,39	0,32
12	0,33	0,16	0,08	0,16	0,08	0,08	0,10	0,17	0,18	0,25	0,34	0,08	0,13	0,18	0,16	0,11	0,22	0,11	0,13	0,12	0,08	0,10	0,18	0,11	0,16	0,20	0,10

Table B.8: Results of each classifier obtained on Data Set C with an epoch of 4s.

Dataset C (epoch 4s)																									
Classifier	GaussianNB			SVM			DTC			RF			KNN			LR			LDA			LSVM			MLP		
Feature Scaling	-	Stand	Norm	-	Stand	Norm	-	Stand	Norm	-	Stand	Norm	-	Stand	Norm	-	Stand	Norm	-	Stand	Norm	-	Stand	Norm	-	Stand	Norm
1	0,20	0,00	0,23	0,00	0,00	0,20	0,20	0,27	0,23	0,20	0,00	0,27	0,00	0,20	0,00	0,20	0,20	0,35	0,20	0,20	0,07	0,16	0,20	0,00	0,00	0,20	0,20
2	0,73	0,45	0,00	0,32	0,47	0,23	0,67	0,45	0,27	0,87	0,33	0,20	0,00	0,27	0,23	0,47	0,59	0,00	0,43	0,45	0,00	0,47	0,32	0,23	0,47	0,32	0,00
3	0,00	0,40	0,23	0,29	0,47	0,52	0,16	0,79	0,27	0,13	0,20	0,36	0,52	0,47	0,23	0,59	0,20	0,27	0,16	0,20	0,53	0,27	0,20	0,52	0,16	0,23	0,32
4	0,32	0,63	0,40	0,32	0,59	0,00	0,00	0,20	0,00	0,32	0,53	0,00	0,32	0,72	0,00	0,32	0,80	0,00	0,32	0,53	0,00	0,32	0,80	0,00	0,20	0,59	0,00
5	0,20	0,20	0,60	0,27	0,27	0,67	0,27	0,27	0,50	0,20	0,53	0,80	0,00	0,00	0,53	0,00	0,27	0,50	0,00	0,27	0,63	0,27	0,00	0,80	0,27	0,20	0,13
6	0,20	0,20	0,20	0,16	0,20	0,20	0,40	0,20	0,27	0,40	0,40	0,20	0,16	0,16	0,27	0,00	0,20	0,47	0,20	0,20	0,47	0,20	0,40	0,47	0,16	0,20	0,47
7	0,00	0,13	0,30	0,00	0,00	0,37	0,20	0,33	0,07	0,27	0,10	0,07	0,00	0,13	0,30	0,13	0,00	0,10	0,00	0,16	0,35	0,00	0,00	0,07	0,00	0,00	0,00
8	0,73	0,00	0,00	0,00	0,67	0,00	0,47	0,80	0,00	0,40	0,40	0,00	0,20	0,36	0,13	0,13	0,33	0,07	0,13	0,13	0,07	0,13	0,13	0,00	0,53	0,40	0,07
9	0,40	0,53	0,27	0,00	0,59	0,20	0,32	0,45	0,20	0,32	0,45	0,00	0,27	0,32	0,40	0,10	0,60	0,27	0,53	0,53	0,27	0,47	0,79	0,27	1,00	0,59	0,27
10	0,36	0,00	0,07	0,00	0,13	0,40	0,36	0,16	0,20	0,36	0,00	0,00	0,27	0,00	0,47	0,27	0,23	0,35	0,27	0,53	0,07	0,27	0,53	0,35	0,16	0,00	0,20
11	0,80	0,59	0,52	0,59	0,80	0,72	0,20	0,59	0,60	0,80	0,80	0,32	0,32	0,80	0,59	0,80	0,80	0,80	0,80	0,80	0,80	0,80	0,80	0,60	0,72	0,80	0,45
12	0,00	0,16	0,08	0,00	0,20	0,00	0,16	0,53	0,00	0,16	0,16	0,00	0,00	0,20	0,00	0,00	0,13	0,10	0,27	0,00	0,13	0,16	0,13	0,00	0,20	0,16	0,10

Table B.9: Results of each classifier obtained on Data Set C with an epoch of 3s.

Dataset C (epoch 3s)																									
Classifier	GaussianNB			SVM			DTC			RF			KNN			LR			LDA			LSVM			MLP		
Feature Scaling	-	Stand	Norm	-	Stand	Norm	-	Stand	Norm	-	Stand	Norm	-	Stand	Norm	-	Stand	Norm	-	Stand	Norm	-	Stand	Norm	-	Stand	Norm
1	0,38	0,23	0,34	0,48	0,25	0,75	0,29	0,00	0,46	0,29	0,23	0,65	0,29	0,38	0,57	0,64	0,48	0,48	0,64	0,52	0,38	0,48	0,64	0,57	0,48	0,49	0,48
2	0,34	0,57	0,13	0,42	0,63	0,00	0,16	0,67	0,00	0,37	0,57	0,10	0,49	0,63	0,33	0,81	0,81	0,13	0,66	0,67	0,13	0,57	0,81	0,14	0,23	0,81	0,07
3	0,19	0,40	0,00	0,07	0,04	0,22	0,22	0,75	0,07	0,23	0,60	0,28	0,45	0,60	0,07	0,05	0,04	0,06	0,04	0,24	0,22	0,05	0,04	0,05	0,07	0,23	0,22
4	0,04	0,04	0,10	0,05	0,04	0,11	0,33	0,04	0,23	0,24	0,22	0,11	0,03	0,03	0,29	0,04	0,04	0,11	0,04	0,04	0,13	0,04	0,04	0,10	0,04	0,04	0,11
5	0,10	0,71	0,04	0,06	0,63	0,04	0,06	0,44	0,27	0,06	0,64	0,04	0,52	0,63	0,04	0,05	0,06	0,04	0,05	0,06	0,04	0,05	0,06	0,04	0,24	0,06	0,04
6	0,71	0,29	0,13	0,40	0,12	0,14	0,17	0,25	0,14	0,17	0,40	0,14	0,18	0,28	0,17	0,21	0,28	0,13	0,23	0,31	0,14	0,22	0,28	0,22	0,75	0,24	0,14
7	0,14	0,00	0,13	0,00	0,20	0,15	0,33	0,60	0,13	0,20	0,37	0,16	0,33	0,33	0,15	0,25	0,42	0,21	0,33	0,20	0,21	0,30	0,42	0,21	0,29	0,25	0,22
8	0,29	0,29	0,00	0,05	0,33	0,07	0,00	0,00	0,23	0,16	0,33	0,04	0,43	0,38	0,46	0,16	0,59	0,16	0,33	0,33	0,04	0,00	0,59	0,10	0,16	0,29	0,19
9	0,29	0,34	0,00	0,28	0,04	0,04	0,59	0,33	0,33	0,48	0,23	0,00	0,61	0,64	0,00	0,28	0,63	0,63	0,28	0,63	0,63	0,43	0,48	0,00	0,74	0,23	0,49
10	0,33	0,37	0,10	0,55	0,12	0,06	0,38	0,29	0,31	0,33	0,38	0,45	0,38	0,43	0,06	0,33	0,35	0,06	0,49	0,37	0,13	0,49	0,58	0,06	0,33	0,37	0,10
11	0,23	0,23	0,42	0,00	0,44	0,37	0,38	0,30	0,54	0,38	0,23	0,37	0,49	0,33	0,57	0,00	0,07	0,37	0,23	0,23	0,37	0,32	0,48	0,23	0,32	0,32	0,00
12	0,05	0,48	0,10	0,00	0,30	0,22	0,17	0,48	0,04	0,24	0,29	0,20	0,08	0,21	0,24	0,13	0,30	0,21	0,13	0,13	0,03	0,13	0,38	0,10	0,13	0,30	0,21

Table B.10: Results of each classifier obtained on Data Set C with an epoch of 2s.

Dataset C (epoch 2s)																									
Classifier	GaussianNB			SVM			DTC			RF			KNN			LR			LDA			LSVM			MLP		
Feature Scaling	-	Stand	Norm	-	Stand	Norm	-	Stand	Norm	-	Stand	Norm	-	Stand	Norm	-	Stand	Norm	-	Stand	Norm	-	Stand	Norm	-	Stand	Norm
1	0,26	0,26	0,12	0,15	0,27	0,18	0,05	0,32	0,16	0,05	0,05	0,25	0,23	0,12	0,13	0,29	0,21	0,24	0,05	0,24	0,24	0,30	0,16	0,24	0,28	0,45	0,24
2	0,35	0,43	0,18	0,45	0,63	0,43	0,26	0,32	0,24	0,53	0,25	0,11	0,25	0,42	0,26	0,39	0,24	0,67	0,29	0,24	0,57	0,22	0,24	0,43	0,39	0,45	0,51
3	0,50	0,50	0,19	0,15	0,21	0,06	0,28	0,28	0,19	0,35	0,35	0,19	0,42	0,42	0,19	0,29	0,29	0,19	0,29	0,29	0,19	0,29	0,29	0,06	0,19	0,21	0,06
4	0,28	0,27	0,07	0,43	0,29	0,23	0,25	0,32	0,07	0,51	0,41	0,21	0,25	0,47	0,07	0,22	0,29	0,07	0,43	0,33	0,21	0,22	0,27	0,07	0,38	0,29	0,07
5	0,12	0,16	0,30	0,16	0,12	0,15	0,28	0,23	0,15	0,41	0,25	0,33	0,29	0,06	0,32	0,20	0,23	0,16	0,18	0,28	0,18	0,12	0,25	0,15	0,15	0,27	0,15
6	0,26	0,48	0,13	0,23	0,42	0,19	0,03	0,31	0,19	0,25	0,53	0,17	0,29	0,20	0,13	0,52	0,13	0,13	0,30	0,18	0,13	0,34	0,18	0,13	0,26	0,13	0,13
7	0,30	0,23	0,17	0,10	0,21	0,29	0,11	0,34	0,14	0,11	0,58	0,29	0,14	0,14	0,18	0,17	0,58	0,30	0,31	0,23	0,25	0,30	0,58	0,29	0,29	0,13	0,29
8	0,14	0,36	0,18	0,23	0,56	0,19	0,08	0,47	0,43	0,08	0,30	0,47	0,32	0,22	0,34	0,47	0,37	0,16	0,25	0,47	0,09	0,30	0,56	0,36	0,27	0,47	0,41
9	0,75	0,26	0,19	0,22	0,58	0,25	0,19	0,41	0,10	0,40	0,27	0,11	0,22	0,28	0,19	0,24	0,57	0,20	0,43	0,57	0,20	0,35	0,57	0,33	0,23	0,48	0,20
10	0,20	0,41	0,17	0,03	0,29	0,19	0,43	0,17	0,17	0,43	0,29	0,32	0,15	0,22	0,06	0,50	0,44	0,17	0,40	0,17	0,30	0,36	0,44	0,17	0,40	0,44	0,18
11	0,39	0,34	0,19	0,18	0,24	0,15	0,21	0,18	0,13	0,42	0,55	0,22	0,19	0,49	0,55	0,16	0,29	0,14	0,31	0,24	0,41	0,28	0,24	0,28	0,22	0,24	0,47
12	0,20	0,27	0,13	0,06	0,18	0,15	0,21	0,19	0,13	0,14	0,24	0,12	0,00	0,33	0,13	0,34	0,38	0,13	0,32	0,27	0,13	0,21	0,27	0,17	0,16	0,34	0,13

Table B.11: Results of each classifier obtained on Data Set D with an epoch of 4s.

Dataset D (epoch 4s)																								
Classifier	GaussianNB			SVM			DTC			RF			KNN			LR			LDA			LSVM			MLP		
Feature Scaling	-	Stand	Norm	-	Stand	Norm	-	Stand	Norm	-	Stand	Norm	-	Stand	Norm	-	Stand	Norm	-	Stand	Norm	-	Stand	Norm	-	Stand	Norm
1	0,79	0,79	0,00	0,79	0,79	0,38	0,79	0,51	0,00	0,71	0,71	0,62	0,79	0,79	0,86	0,79	0,69	0,57	0,79	0,86	0,43	0,79	0,78	0,57	0,79	0,38	0,57
2	0,00	0,57	0,60	0,60	0,52	0,52	0,52	0,48	0,59	0,52	0,48	0,61	0,60	0,43	0,60	0,52	0,57	0,61	0,52	0,65	0,47	0,52	0,57	0,61	0,52	0,48	0,47
3	0,34	0,71	0,19	0,42	0,34	0,38	0,54	0,38	0,54	0,65	0,54	0,38	0,42	0,52	0,60	0,54	0,34	0,57	0,46	0,54	0,52	0,65	0,34	0,57	0,65	0,43	0,47
4	0,42	0,42	0,42	0,42	0,42	0,42	0,42	0,34	0,42	0,42	0,42	0,42	0,42	0,42	0,42	0,42	0,42	0,42	0,42	0,42	0,43	0,42	0,42	0,42	0,42	0,42	0,42
5	0,75	0,85	0,18	0,71	0,71	0,71	0,70	0,87	0,50	0,70	0,71	0,72	0,71	0,71	0,71	0,75	0,80	0,53	0,75	0,85	0,53	0,16	0,90	0,75	0,70	0,85	0,57
6	0,31	0,55	0,36	0,52	0,62	0,36	0,40	0,79	0,37	0,53	0,70	0,34	0,41	0,49	0,29	0,41	0,79	0,37	0,41	0,60	0,45	0,26	0,66	0,37	0,43	0,79	0,08
7	0,38	0,40	0,49	0,36	0,38	0,38	0,36	0,54	0,30	0,38	0,36	0,46	0,38	0,51	0,38	0,38	0,38	0,38	0,36	0,40	0,54	0,34	0,38	0,60	0,25	0,38	0,38
8	0,04	0,87	1,00	0,79	0,79	0,71	0,79	0,71	0,62	0,79	0,79	0,71	0,79	0,79	0,79	0,79	0,79	0,79	0,79	1,00	0,62	0,04	1,00	0,71	0,79	0,92	0,71
9																											
10																											
11	0,65	0,67	0,16	0,61	0,57	0,65	0,65	0,64	0,60	0,60	0,61	0,42	0,61	0,57	0,57	0,61	0,61	0,45	0,65	0,77	0,36	0,74	0,61	0,52	0,61	0,60	0,52
12	0,61	0,68	0,14	0,00	0,57	0,54	0,57	0,60	0,39	0,45	0,57	0,36	0,61	0,57	0,31	0,61	0,61	0,33	0,61	0,61	0,36	0,02	0,61	0,46	0,61	0,65	0,46

Table B.12: Results of each classifier obtained on Data Set D with an epoch of 3s.

Dataset D (epoch 3s)																								
Classifier	GaussianNB			SVM			DTC			RF			KNN			LR			LDA			LSVM			MLP		
Feature Scaling	-	Stand	Norm	-	Stand	Norm	-	Stand	Norm	-	Stand	Norm	-	Stand	Norm	-	Stand	Norm	-	Stand	Norm	-	Stand	Norm	-	Stand	Norm
1	0,87	0,77	0,02	0,87	0,82	0,61	0,87	0,82	0,00	0,86	0,82	0,81	0,87	0,82	0,87	0,87	0,77	0,81	0,87	0,82	0,81	0,87	0,77	0,86	0,87	0,82	0,68
2	0,02	0,39	0,36	0,23	0,35	0,45	0,18	0,25	0,43	0,13	0,39	0,44	0,23	0,23	0,49	0,18	0,25	0,23	0,23	0,25	0,49	0,23	0,25	0,26	0,23	0,25	0,49
3	0,42	0,41	0,42	0,23	0,34	0,09	0,28	0,36	0,15	0,39	0,35	0,29	0,42	0,35	0,10	0,44	0,42	0,42	0,44	0,49	0,42	0,27	0,49	0,43	0,47	0,37	0,16
4	0,40	0,45	0,27	0,45	0,45	0,40	0,40	0,28	0,62	0,45	0,45	0,59	0,45	0,45	0,45	0,45	0,45	0,45	0,45	0,45	0,30	0,40	0,45	0,40	0,45	0,45	0,45
5	0,01	0,49	0,32	0,50	0,47	0,41	0,47	0,61	0,30	0,59	0,50	0,32	0,50	0,47	0,51	0,47	0,49	0,36	0,50	0,47	0,38	0,37	0,47	0,43	0,47	0,49	0,43
6	0,53	0,53	0,40	0,56	0,63	0,37	0,56	0,58	0,43	0,67	0,60	0,44	0,63	0,65	0,40	0,55	0,57	0,38	0,55	0,53	0,24	0,43	0,66	0,38	0,36	0,60	0,40
7	0,63	0,72	0,00	0,70	0,72	0,19	0,62	0,69	0,07	0,69	0,69	0,21	0,72	0,70	0,30	0,60	0,72	0,17	0,56	0,72	0,10	0,32	0,63	0,26	0,49	0,66	0,12
8	0,16	0,66	0,66	0,58	0,58	0,60	0,47	0,75	0,43	0,53	0,75	0,48	0,47	0,58	0,58	0,53	0,58	0,73	0,66	0,89	0,55	0,56	0,75	0,73	0,58	0,75	0,58
9																											
10																											
11	0,31	0,67	0,35	0,71	0,74	0,71	0,81	0,60	0,42	0,81	0,70	0,62	0,70	0,70	0,67	0,73	0,71	0,71	0,78	0,68	0,43	0,36	0,71	0,60	0,71	0,70	0,71
12	0,07	0,42	0,45	0,41	0,41	0,39	0,41	0,47	0,48	0,43	0,34	0,40	0,41	0,38	0,41	0,41	0,41	0,41	0,41	0,42	0,36	0,47	0,42	0,39	0,52	0,42	0,41

Table B.13: Results of each classifier obtained on Data Set D with an epoch of 2s.

Dataset D (epoch 2s)																								
Classifier	GaussianNB			SVM			DTC			RF			KNN			LR			LDA			LSVM			MLP		
Feature Scaling	-	Stand	Norm	-	Stand	Norm	-	Stand	Norm	-	Stand	Norm	-	Stand	Norm	-	Stand	Norm	-	Stand	Norm	-	Stand	Norm	-	Stand	Norm
1	0,65	0,76	0,34	0,68	0,68	0,68	0,75	0,66	0,33	0,67	0,68	0,57	0,79	0,68	0,68	0,65	0,68	0,68	0,65	0,65	0,58	0,06	0,65	0,69	0,68	0,65	0,68
2	0,53	0,68	0,11	0,70	0,60	0,76	0,70	0,74	0,41	0,65	0,71	0,21	0,69	0,52	0,40	0,70	0,72	0,76	0,63	0,65	0,01	0,36	0,75	0,11	0,53	0,50	0,76
3	0,49	0,55	0,02	0,51	0,54	0,02	0,53	0,56	0,14	0,43	0,53	0,30	0,48	0,58	0,23	0,58	0,55	0,02	0,56	0,56	0,12	0,49	0,55	0,13	0,56	0,59	0,14
4	0,57	0,63	0,36	0,62	0,59	0,36	0,57	0,66	0,51	0,60	0,63	0,51	0,57	0,66	0,55	0,57	0,66	0,31	0,62	0,60	0,36	0,62	0,63	0,62	0,48	0,63	0,66
5	0,25	0,46	0,34	0,38	0,38	0,38	0,41	0,46	0,44	0,41	0,42	0,43	0,39	0,46	0,50	0,41	0,38	0,36	0,40	0,47	0,37	0,37	0,46	0,38	0,38	0,38	0,38
6	0,45	0,62	0,50	0,55	0,56	0,57	0,40	0,48	0,41	0,57	0,63	0,56	0,50	0,51	0,49	0,56	0,64	0,51	0,47	0,59	0,52	0,34	0,56	0,59	0,43	0,67	0,59
7	0,42	0,41	0,31	0,41	0,41	0,45	0,38	0,47	0,40	0,38	0,41	0,52	0,41	0,39	0,42	0,39	0,41	0,39	0,41	0,40	0,51	0,28	0,42	0,48	0,43	0,41	0,40
8	0,15	0,75	0,25	0,53	0,53	0,53	0,68	0,51	0,36	0,53	0,53	0,55	0,53	0,53	0,53	0,59	0,53	0,53	0,56	0,51	0,57	0,24	0,51	0,46	0,53	0,53	0,53
9																											
10																											
11	0,57	0,58	0,53	0,61	0,56	0,55	0,55	0,67	0,53	0,63	0,54	0,52	0,65	0,62	0,56	0,55	0,55	0,55	0,63	0,62	0,21	0,55	0,55	0,55	0,68	0,55	0,55
12	0,12	0,56	0,39	0,52	0,52	0,53	0,52	0,51	0,27	0,57	0,56	0,27	0,52	0,50	0,36	0,53	0,52	0,37	0,57	0,60	0,35	0,59	0,55	0,51	0,53	0,49	0,57